1   **The Influence of Carbon Cycling on Oxygen Depletion in North-Temperate Lakes**
2

3   Austin Delany[1], Robert Ladwig[1], Cal Buelo[1], Ellen Albright[1], Paul C. Hanson[1]

4   [1] Center for Limnology, University of Wisconsin-Madison, Madison, WI, USA

5   *Correspondence to*: Austin Delany (addelany@wisc.edu)

6

7   **Abstract.** Hypolimnetic oxygen depletion during summer stratification in lakes can lead to

8   hypoxic and anoxic conditions. Hypolimnetic anoxia is a water quality issue with many

9   consequences, including reduced habitat for cold-water fish species, reduced quality of

10   drinking water, and increased nutrient and organic carbon (OC) release from sediments. Both

11   allochthonous and autochthonous OC loads contribute to oxygen depletion by providing

12   substrate for microbial respiration; ~~however, their relative importance in depleting oxygen~~

13   ~~across diverse lake systems remains uncertain~~ however, their relative contributions to oxygen

14   depletion across diverse lake systems remains uncertain. Lake characteristics, such as trophic

15   state, hydrology, and morphometry are also influential in carbon cycling processes and may

16   impact oxygen depletion dynamics. To investigate the effects of carbon cycling on

17   hypolimnetic oxygen depletion, we used a two-layer process-based lake model to simulate

18   daily metabolism dynamics for six Wisconsin lakes over twenty years (1995-2014). Physical

19   processes and internal metabolic processes were included in the model and were used to

20   predict dissolved oxygen (DO), particulate OC (POC), and dissolved OC (DOC). In our

21   study of oligotrophic, mesotrophic, and eutrophic lakes, we found autochthony to be far more

22   important than allochthony to hypolimnetic oxygen depletion. Autochthonous POC

23   respiration in the water column contributed the most towards hypolimnetic oxygen depletion

24   in the eutrophic study lakes. POC water column respiration and sediment respiration had

25   similar contributions in the mesotrophic and oligotrophic study lakes. Differences in source

26   of respiration are discussed with consideration of lake productivity and the processing and

27   fates of organic carbon loads.

28
29
30
31
32
33
34
35
36
37
38
39
40
41
42
43
44
45
46
47
48
49
50
51
52
53
54
55
56
57
58
59
60
61
62
63
64
65

1 Introduction

Hypolimnetic oxygen depletion is a persistent and global phenomenon that degrades lake ecosystems services (Nürnberg 1995; Cole & Weihe 2016; Jenny et al. 2016). In lakes where oxygen depletion results in hypoxia and even anoxia, habitat availability for cold-water fish species is eliminated (Magee et al. 2019), quality of drinking water is reduced (Bryant et al. 2011), and nutrient and OC release from lake sediments becomes elevated (Hoffman et al. 2013, McClure et al. 2020). An increase in the prevalence of hypolimnetic anoxia and associated water quality degradation in temperate lakes indicates the need to better understand how lake ecological processes interact with external forcings, such as hydrology and nutrient inputs, to control the development of anoxia (Jenny et al, 2016 a,b).

Allochthonous organic carbon (OC) loading to lakes that explains the prevalence of negative net ecosystem production (i.e., net heterotrophy) provides substrate for hypolimnetic oxygen depletion (Houser et al. 2003). Allochthonous OC sources have also been shown to influence dissolved oxygen (DO) and carbon dynamics in lakes by providing recalcitrant substrate for respiration (Cole et al. 2002; Hanson et al. 2014, Solomon et al. 2015). In lake surveys, dissolved allochthonous OC correlates positively with net heterotrophy ((Jansson et al. 2000), indicating the importance of allochthony to both the carbon balance and dynamics of dissolved gases (Prairie et al. 2002; Hanson et al. 2003). However, the persistent and often stable concentration of allochthonous DOC in the water column of lakes also indicates its recalcitrant nature, raising the question of whether allochthony alone can support high oxygen demand in the sediments and deeper waters of lakes.

3

90   The contributions of OC from autochthony to hypolimnetic oxygen depletion may be

91   important as well, despite its low concentrations relative to that of allochthonous OC in many

92   lakes (Cole et al. 2002). Autochthonous OC tends to be highly labile (Amon & Brenner 1996,

93   Thorpe & Delong 2002), and spot samples from lake surveys may not detect autochthonous

94   DOC, reducing its power as a correlate of ecosystem function. Positive correlation between

95   anoxia and lake phosphorus concentrations suggests autochthony may contribute

96   substantially to hypolimnetic oxygen demand (Rhodes et al. 2017; Rippey & McSorley,

97   2009; Jenny et al. 2016a,b); however, the link between nutrient concentrations, autochthony,

98   and hypolimnetic respiration is rarely quantified. Lakes with high autochthony can still be net

99   heterotrophic (Staehr et al. 2010; Cole et al. 2000), however, it matters where in the lake

100   autochthony is respired. Export of phytoplankton from the epilimnion to the hypolimnion and

101   sediments contributes to deep water oxygen demand (Müller et al. 2012; Rhodes et al. 2017;

102   Beutel 2003), and the magnitude and timing of organic carbon inputs to deeper waters in

103   lakes and the subsequent fate of that carbon deserves further exploration.

104
105   Understanding the relative ~~importance~~ contributions of autochthony and allochthony to

106   hypolimnetic oxygen depletion requires consideration of a number of physical and biological

107   processes controlling oxygen sources and sinks in lakes (Hanson et al. 2015). For dimictic

108   north temperate lakes, the timing and dynamics of seasonal stratification determine the

109   ambient temperature and light conditions for metabolism and the extent to which the

110   hypolimnion is isolated from oxygen-rich surface waters (Snortheim et al. 2017, Ladwig et

111   al. 2021). In many lakes, the hypolimnion is below the euphotic zone, but in very clear lakes,

112   primary production within the hypolimnion may be an oxygen source (Houser et al. 2003).

4

113   Lake morphometry influences the spatial extents of stratified layers, which determines the

114   ratio of hypolimnetic volume to sediment surface area and the magnitude the sediment

115   oxygen sink for the hypolimnetic oxygen budget (Livingstone & Imboden 1996). Thus, the

116   sources and labilities of OC, lake morphometry, and lake hydrodynamics all contribute to

117   hypolimnetic oxygen budgets, making it an emergent ecosystem property with a plethora of

118   causal relationships to other ecologically important variables.

119
120   The availability of long-term observational data combined with process-based models

121   provides an opportunity to investigate OC sources and their control over the dynamics of lake

122   DO across multiple time scales. Long-term studies of lakes on regional and global scales

123   highlight how environmental trends can influence metabolic processes in lakes, and how

124   lakes can broaden our understanding of large-scale ecosystem processes (Richardson et al.

125   2017, Kraemer et al. 2017, Williamson et al. 2008). For example, long-term studies allow us

126   to investigate the impact that current and legacy conditions have on lake ecosystem function

127   in a given year (Carpenter et al. 2007). Process-based modeling has been used to investigate

128   metabolism dynamics and understand both lake carbon cycling (Hanson et al. 2004, Cardille

129   et al. 2007) and formation of anoxia (Ladwig et al. ~~2022~~ 2021); however, explicitly tying

130   lake carbon cycling and metabolism dynamics with long-term hypolimnetic DO depletion

131   across a variety of lakes remains largely unexplored. The combination of process-based

132   modeling with available long-term observational data, including exogenous driving data

133   representative of climate variability, can be especially powerful for recreating representations

134   of long-term lake metabolism dynamics (Staehr et al. 2010, Cardille et al. 2007).

135

5

136 In this study, our goal is to investigate OC source contributions to lake carbon cycling and

137 hypolimnetic oxygen depletion. The importance of excess primary production to anoxia has

138 been established (Nürnberg et al. 1995, Müller et al. 2012). We build upon this research by

139 quantifying the timing and magnitude of OC contributions to hypolimnetic anoxia. We are

140 particularly interested in the relative loads of autochthonous and allochthonous OC to lakes

141 and how they contribute to hypolimnetic DO depletion across seasonal to decadal scales. We

142 use a process-based lake metabolism model, combined with daily external driving data and

143 long-term limnological data, to study six lakes within the North Temperate Lakes Long-Term

144 Ecological Research network (NTL LTER) over a twenty-year period (1995-2014). We

145 address the following questions: (1) What are the dominant sources of organic carbon that

146 contribute to hypolimnetic oxygen depletion, and how do their contributions differ across a

147 group of diverse lakes over two decades? (2) How does lake trophic state influence the

148 processing and fates of organic carbon loads in ways that affect hypolimnetic dissolved

149 oxygen?

150

151 **2 Methods**

152 **2.1 Study Site**

153 This study includes six Wisconsin lakes from the NTL-LTER program (Magnuson et al.

154 2006). Trout Lake (TR), Big Muskellunge Lake (BM), Sparkling Lake (SP), and Allequash

155 Lake (AL) are in the Northern Highlands Lake District of Wisconsin and have been regularly

156 sampled since 1981 (Magnuson et al. 2006). Lake Mendota (ME) and Lake Monona (MO)

157 are in southern Wisconsin and have been regularly sampled by the NTL-LTER since 1995

158   (NTL-LTER, Magnuson et al. 2006). The NTL-LTER provides a detailed description of each

159   lake (Magnuson et al. 2006). The six lakes span gradients in size, morphometry, landscape

160   setting, and hydrology, which creates diverse carbon cycling characteristics and processes

161   across these systems. TR and AL are drainage lakes with high allochthonous carbon inputs

162   from surface water, while BM and SP are groundwater seepage systems with allochthony

163   dominated by aerial OC inputs from the surrounding landscape (Hanson et al. 2014). All four

164   northern lakes (TR, AL, BM, SP) are surrounded by a forested landscape. ME and MO are

165   both eutrophic drainage lakes surrounded by an urban and agricultural landscape. Although

166   the full range of DOC concentrations for lakes in northern Wisconsin varies from about 2 to

167   >30 mg L^{-1} (Hanson et al. 2007), DOC concentrations among our study lakes covered a

168   relatively narrow range typical of non-dystrophic lakes in Wisconsin (Hanson et al. 2007)

169   and are near the global averages previously estimated, i.e., 3.88 mg/L (Toming et al. 2020)

170   and 5.71 mg/L (Sobek et al. 2007), respectively. Morphometry, hydrology, and other

171   information can be found in Table 1.

172
173
174
175
176
177
178
179
180
181
182
183

7

184 **Table 1.** Physical and biogeochemical characteristics of the study lakes. The table includes
185 lake area (Area), maximum depth (Zmax), hydrologic residence time (RT), mean annual
186 temperature (Temp), mean annual surface total phosphorus concentration (Mean TP), and
187 mean annual surface DOC (Mean DOC).
188

Lake	Area (ha)	Zmax (m)	RT [3,4] (years)	Temp [2] (°C)	Mean TP [1] (µgL)	Mean DOC [1] (mgL)
Allequash Lake (AL)	168.4	8	0.73	10.5	14	3.9
Big Muskellunge (BM)	396.3	21.3	5.1	10.5	7	3.8
Sparkling Lake (SP)	64	20	8.88	10.6	5	3.12
Trout Lake (TR)	1607.9	35.7	5.28	9.8	5	2.8
Mendota (ME)	3961	25.3	4.3	12.5	50	5.6
Monona (MO)	1324	22.5	0.7	13.8	47	5.8

189
190 1 - Magnuson et al. (2020, 2006)
191 2 - Magnuson et al. (2022)
192 3 - Hunt et al. (2013)
193 4 - Webster et al. (1996)
194

195

196 **2.2 Driving Data and Limnological Data**

197 Most driving data for the model is provided by the "Process-based predictions of water

198 temperature in the Midwest US" USGS data product (Read et al. 2021). This includes lake

199 characteristic information such as lake area and hypsometry, daily modeled temperature

8

200   profiles, ice flags, meteorology data, and solar radiation for the six study lakes. Derived

201   hydrology data is used in calculating daily OC loading and outflow for the study lakes.

202   Hydrology for the northern lakes is taken from Hunt & Walker (2017), which was estimated

203   using a surface and groundwater hydrodynamic model. Hydrology for ME is taken from

204   Hanson et al. (2020), which used the Penn State Integrated Hydrologic Model (Qu & Duffy

205   2007). We assume for ME and MO that evaporation from the lake surface is approximately

206   equal to precipitation on the lake surface and that groundwater inputs and outputs to the lake

207   are a small part of the hydrologic budgets (Lathrop & Carpenter 2014). Therefore, ME

208   outflow is assumed to be equal to ME inflow. ME is the predominant hydrologic source for

209   MO (Lathrop & Carpenter 2014), thus, MO inflow is assumed to be equal to ME outflow,

210   and MO outflow is assumed to be equal to MO inflow. We found that the derived discharge

211   data for ME, TR, AL, and SP was approximately 20-50% higher than previously reported

212   values (Hunt et al. 2013, Webster et al. 1996), depending on the lake, while hydrology in BM

213   was approximately 25% too low (Hunt et al. 2013). To accommodate this issue, we adjusted

214   total annual hydrological inputs to match published water residence times for each lake

215   (Table 1), while retaining temporal hydrological patterns. NTL-LTER observational data are

216   interpolated to estimate daily nutrient concentration values, which are used in calculating

217   daily primary production in the model (Magnuson et al. 2020).

218

219   The NTL-LTER observational data used to calibrate and validate the model for the six lakes

220   include DO, DOC, and Secchi depth (Magnuson et al. 2020, Magnuson et al. 2022).

221   Saturation values for DO and gas exchange velocity used in calculating atmospheric

9

222   exchange for DO are calculated using the "o2.at.sat.base" and using the Cole and Caraco gas

223   exchange method from the "K600.2.KGAS.base" function within the USGS

224   "LakeMetabolizer" package in R (Winslow et al. 2016).

225

226   **2.3 The Model**

227   The goal of our model is to use important physical and metabolic processes involved in the

228   lake ecosystem carbon cycle to best predict DO, DOC, and POC, while keeping the model

229   design simple in comparison with more comprehensive water quality models (e.g., Hipsey et

230   al. 2022). We ran our model with a daily time step over a twenty-year period (1995-2014) for

231   each lake and included seasonal physical dynamics, such as lake mixing, stratification, and

232   ice cover from Read et al. 2021. Throughout each year, the model tracks state variables and

233   fluxes in the lake for each day (Fig. 1). These state variables include DO and the labile and

234   recalcitrant components of particulate organic carbon (POC) and dissolved organic carbon

235   (DOC). Initial conditions for each state variable are based on literature values or lake

236   observational data (SI Table 5). The model is initialized on January 1st of the first year, so

237   we set the initial labile POC mass to zero under the assumption that the concentration is low

238   in the middle of winter. The initial DO value is set to the saturation value based on the

239   conditions of the initial model run day and is calculated using the LakeMetabolizer R

240   package (Winslow et al. 2016). During stratified periods, the state variables and fluxes for

241   the epilimnion and hypolimnion are tracked independently. Atmosphere, sediments, and

242   hydrologic inputs and outputs are boundary conditions.

243
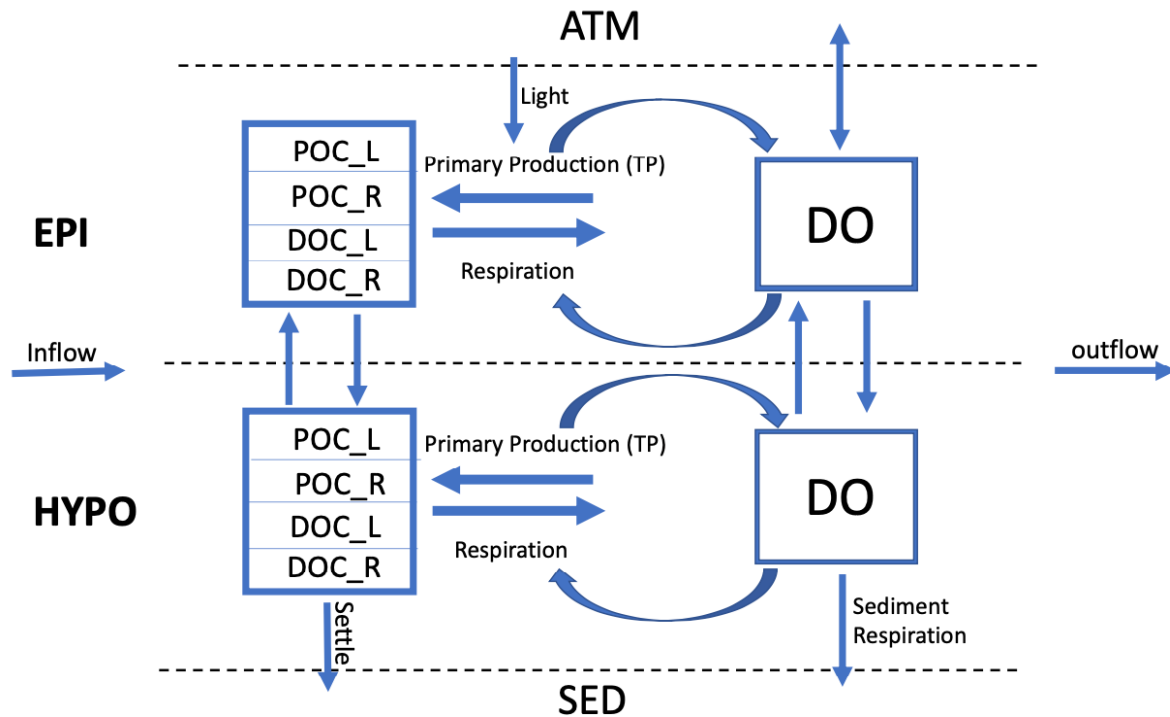
Figure 1. Conceptual lake model showing state variables (boxes) and fluxes (arrows). The model has two thermal layers under stratified conditions, as shown here, and tracks state variables separately for each layer. The sediment (SED), atmosphere (ATM), inflow and outflow are system boundaries. The state variables included are DO (dissolved oxygen), DOC_L (labile dissolved organic carbon), DOC_R (recalcitrant dissolved organic carbon), POC_L (labile particulate organic carbon), and POC_R (recalcitrant particulate organic carbon). Observed total phosphorus (TP) is used as a driving variable for primary production in the model.

The model is built specifically for this analysis; however, many of the assumptions around the model complexity and mathematical formulations are borrowed from literature cited (Ladwig et al. ~~2022~~ 2021, Hipsey et al. 2022, Hanson et al. 2014, McCullough et al. 2018). ~~We chose to develop our own process-based model rather than use an existing model, such as GLM (Hipsey et al. 2022) or Simstrat (Goudsmit et al. 2002), so that we could simulate and measure the specific metabolism fluxes related to our study questions.~~ We chose to develop our own process-based model for water quality rather than use an existing model, such as GLM-AED2 (Hipsey et al. 2022; note that AED2 is the water quality component of the

11

262　coupled hydrodynamic-water quality model) or Simstrat (Goudsmit et al. 2002), so that we

263　could simulate and measure the specific metabolism fluxes related to our study questions. We

264　used a pre-existing dataset (Read et al. 2021) that provided GLM modeled daily water

265　temperature profiles for our study lakes, however our study did not use any established water

266　quality models to calculate the relative OC or DO pools.

267

268

269　**2.3.1 Stratification Dynamics**

270　Lake physical dynamics are taken from the output of a previous hydrodynamic modeling

271　study on these same lakes over a similar time period (Read et al. 2021), which used the

272　General Lake Model (Hipsey et al. 2019). Before running the metabolism model, a

273　thermocline depth for each time step is estimated using derived temperature profiles for each

274　lake (Read et al. 2021) by determining the center of buoyancy depth (Read et al. 2011). After

275　calculating the thermocline depth, the volumes and average temperatures for each layer, and

276　the specific area at thermocline depth are determined using lake-specific hypsography. The

277　criteria for stratification include a vertical density gradient between the surface and bottom

278　layer of at least 0.05 kg m^{-3}, an average water column temperature above 4 °C, and the

279　presence of a derived thermocline (Ladwig et al. ~~2022~~ 2021). For any day that does not meet

280　all of these criteria, the water column is considered to be fully mixed. The thermocline depth

281　values are smoothed using a moving average with a window size of 14 days to prevent large

282　entrainment fluxes that can destabilize the model at very short time scales when thermal

283　strata are shallow. During mixed periods, the entire lake is treated as the epilimnion, and a

12

284   separate hypolimnion is not incorporated into the model dynamics. Ice cover in the model is

285   determined using the "ice flag" provided in the derived temperature profile data from Read et

286   al. (2021). Our metabolism model does simulate under-ice conditions, however we do not

287   include the presence of inverse stratification during winter periods.

288

13

2.3.2 External Lake and Environment Physical Fluxes

Atmospheric exchange of DO, external loading of OC, and outflow of OC are the three

environmental boundary fluxes accounted for in the water quality model (Table 2 Eq. 9-11).

The gas exchange velocity for atmospheric exchange is determined using the Cole and

Caraco model (1998) and is calculated using the LakeMetabolizer R package (Winslow et al.

2016). Oxygen saturation values are also calculated using this package. During ice covered

conditions, we assume that the atmospheric exchange value is ten percent of the value during

non-ice covered conditions based on sea ice gas exchange estimates (Loose and Schlosser,

2011).

For the northern lakes (TR, AL, BM, SP), we assume that allochthonous OC loads consist of

entirely recalcitrant substrates. We verify total OC load, total inflow concentration, and

recalcitrant OC export values with estimates from Hanson et al. (2014). For ME, we verify

the total annual allochthonous OC load and OC inflow concentrations against observed

inflow data from Hart et al. (2017) by back calculating inflow concentrations based on the

modeled OC equilibrium of the lake. MO inflow concentrations are equivalent to the in-lake

epilimnetic concentrations of OC from ME at each model time step. The total OC loads for

MO are verified based on the total allochthonous load found in McCullough et al. 2018.

Table 2. Equations for the model, organized by state variables, [DO (dissolved oxygen),
$DOCL$ (labile dissolved organic carbon), $DOCR$(recalcitrant dissolved organic carbon),
$POCL$ (labile particulate organic carbon), $POCR$ (recalcitrant particulate organic carbon),
$Secchi$] and relevant fluxes. *Note:* The entrainment flux ($Entr$) is only included during
thermally stratified periods. The inflow (IN) and outflow (OUT) fluxes are not included in
the calculations for the hypolimnetic layer. The inflow of labile DOC (IN_{DOCL}) parameter in
Eq. 2 is only used for calculating allochthonous OC loads for MO. Atmospheric gas

14

exchange of dissolved oxygen (*AtmExch*) is not included for the hypolimnetic DO
calculation. Normalized total phosphorus is represented by (*TP$_{norm}$*). The volume (*V*) term
represents the respective lake layer volume, or the discharge volume for the inflow and
outflow equations. The term (*r$_{rate}$*) is included in Eq. 13 to represent the respiration rates of
the different OC pools. It is included to simplify the table of equations. Terms not defined
here are included in Table 3.

State Variables	
DO [gDO] $$\frac{dDO}{dt} = (NPP * O2_{convert}) + AtmExch + Entr_{DO} - (R_{sed} * O2_{convert}) - (R_{wc} * O2_{convert})$$	(1)
DOCL [gC] $$\frac{dDOC_L}{dt} = (NPP * (1 - C_{NPP})) + IN_{DOCL} + Entr_{DOCL} - R_{DOCL} - OUT_{DOCL}$$	(2)
DOCR [gC] $$\frac{dDOC_R}{dt} = IN_{DOCR} + Entr_{DOCR} - OUT_{DOCR} - R_{DOCR\ Epi}$$	(3)
POCL [gC] **Mixed and Epi:** $\frac{dPOC_L}{dt} = (NPP_{Epi} * C_{NPP}) + IN_{POCL} + Entr_{POCL} - R_{POCL\ Epi} - Settle_{POCL\ Epi} - OUT_{POCL}$	(4)
Hypo: $\frac{dPOC_L}{dt} = (NPP_{Hypo} * C_{NPP}) + Settle_{POCL\ Epi} - Settle_{POCL\ Hypo} - R_{POCL\ Hypo} - Ent_{POCL}$	(5)
POCR [gC] **Mixed and Epi:** $\frac{dPOC_R}{dt} = IN_{POCR} + Entr_{POCR} - OUT_{POCR} - R_{POCR\ Epi} - Settle_{POCR\ Epi}$	(6)
Hypo: $\frac{dPOC_R}{dt} = Settle_{POCR\ Epi} - Settle_{POCR\ Hypo} - R_{POCR\ Hypo} - Entr_{POCR}$	(7)
Secchi [m] $$Secchi = \frac{1.7}{K_{LEC}}$$	(8)
Fluxes	
Atm exchange [gDO d^{-1}] $$AtmExch = K_{DO} * (DO_{sat} - DO_{prediction}) * Area_{sfc}$$	(9)
Inflow [gC d^{-1}] $$IN = Carbon\ Concentration_{inflow} * V_{inflow}$$	(10)
Outflow [gC d^{-1}] $$OUT = Carbon\ Concentration_{outflow} * V_{outflow}$$	(11)
Net Primary Productivity [gC d^{-1}] $$NPP = Pmax * (1 - e^{(-IP * \frac{Light}{Pmax})}) * TP_{norm} * \theta_{NPP}^{(T-20)} * V$$	(12)
Respiration [gC d^{-1}] $$R_{wc} = Carbon\ Pool * r_{rate} * \theta_{Resp}^{(T-20)} * \frac{DO_{Concentration}}{DO_{1/2} + DO_{Concentration}}$$	(13)
Sediment Respiration [gC d^{-1}] $$R_{sed} = r_{sed} * \theta_{Resp}^{(T-20)} * \frac{DO_{Concentration}}{DO_{1/2} + DO_{Concentration}} * Area_{sed}$$	(14)
POC settle [gC d^{-1}] $$Settle = (POC\ Pool * K_{POC}) * \frac{Area}{V}$$	(15)

15

Entrainment [gC d^{-1}]	
$V_{Entr} = V_{epi}(t) - V_{epi}(t-1)$	(16)
$V_{Entr} > 0$ (Epilimnion growing)	
$\quad Entr = \frac{V_{Entr}}{V_{Hypo}} * Carbon\ Pool_{Hypo}$	(17)
$V_{Entr} < 0$ (Epilimnion shrinking)	
$\quad Entr = \frac{V_{Entr}}{V_{Epi}} * Carbon\ Pool_{Epi}$	(18)
Light [W m^{-2}]	
$Light = \int_{z_1}^{z_2}(I_{z_1} * e^{-(K_{LEC} * z)})\,dz * (1-\alpha)$	(19)
Light Extinction Coefficient [Unitless]	
$K_{LEC} = LEC_{water} + (LEC_{POC} * ((\frac{POCL}{V}) + (\frac{POCR}{V}))) + (LEC_{DOC} * ((\frac{DOCL}{V}) + (\frac{DOCR}{V})))$	(20)

322

2.3.3 Internal Lake Physical Fluxes

The two in-lake physical fluxes included in the model are POC settling and entrainment of all

state variables. POC settling is the product of a sinking rate (m d^{-1}) and the respective POC

pool (g), divided by the layer depth (m) (Table 2 Eq. 15). Sinking rates are either borrowed

from literature values (Table 3) or fit during model calibration (see below). Entrainment is

calculated as a proportion of epilimnetic volume change (Table 2 Eq. 17-18). A decrease in

epilimnetic volume shifts mass of state variables from the epilimnion into the hypolimnion,

and an increase in volume shifts mass from the hypolimnion to the epilimnion.

16

334 **Table 3.** Model Parameters, grouped into three categories: constants, which are values that
335 were not tuned; manually calibrated, which are parameters manually tuned, typically guided
336 by ranges from the literature; and parameters calibrated through constrained parameter
337 search, which are calibrated through an automated search of parameter space.
338

Parameter	Abbreviation	Value	Units	Source
Constants				
Conversion of Carbon to Oxygen	$O2_{convert}$	2.67	Unitless	Mass Ratio of C:O
Respiration rate of DOCR	r_{DOCR}	0.001	day^{-1}	(Hanson et al., 2011)
Respiration rate of POCR	r_{POCR}	0.005	day^{-1}	Taken from ranges provided in (Hanson et al. 2004)
Respiration rate of POCR	r_{POCR}	0.005	day^{-1}	Taken from ranges provided in (Hanson et al. 2004)
Respiration rate of POCL	r_{POCL}	0.2	day^{-1}	Taken from ranges provided in (Hipsey et al. 2022)
Michaelis-Menten DO half saturation coefficient	$DO_{1/2}$	0.5	$g^{-}m^{-3}$	Taken from ranges provided in (Hipsey et al. 2022)
Light extinction coefficient of water	LEC_{water}	0.125	m^{-1}	Taken from ranges in Hart et al. (2017)
Ratio of DOC to POC production from NPP	C_{NPP}	0.8	Unitless	Biddanda & Benner (1997)
Albedo	α	0.3	Unitless	Global average (Marshall & Plumb, 2008)
Atmospheric gas exchange adjustment during ice covered conditions	C_{winter}	0.1	Unitless	Taken from ranges in (Loose & Schlosser, 2011)
Coefficient of light transmitted through ice	C_{ice}	0.05	Unitless	Taken from ranges provided in (Lei et al. 2011)
Settling velocity rate of POC_R	K_{POCR}	1.2	$m^{-}day^{-1}$	Taken from ranges found in (Reynolds et al.1987)

17

Parameter	Abbreviation	Value	Units	Source
Settling velocity rate of POC_L	K_{POCL}	1	$m-day^{-1}$	Taken from ranges ranges found in (Reynolds et al.1987)
Temperature scaling coefficient for NPP	θ_{NPP}	1.12	Unitless	Taken from values provided in (Hipsey et al. 2022) and (Ladwig et al. 2022 2021)
Temperature scaling coefficient for Respiration	θ_{Resp}	1.04	Unitless	Taken from values provided in (Hipsey et al. 2022) and (Ladwig et al. 2022 2021)
Manually calibrated				
Light extinction of DOC	LEC_{DOC}	0.02 - 0.06	$m^2 g^{-1}$	Manually calibrated based on observed Secchi Depth ranges for the study lakes
Light extinction of POC	LEC_{POC}	0.7	$m^2 g^{-1}$	Manually calibrated based on observed Secchi Depth ranges for the study lakes
Maximum Daily Productivity	$Pmax$	0.5-5	$g-m^{-3}day^{-1}$	Manually calibrated from mean productivity values from Wetzel (2001)
Recalcitrant DOC inflow concentration	$DOCR_{inflow}$	5-10	$g-m^{-3}$	Based on ranges found in (Hanson et al. 2014, McCullough et al. 2018, Hart et al. 2017)
Recalcitrant POC inflow concentration	$POCR_{inflow}$	2-5	$g-m^{-3}$	Based on ranges found in (Hanson et al. 2014, McCullough et al. 2018, Hart et al. 2017)
Calibrated through constrained parameter search				
Slope of the irradiance/productivity curve	IP	0.045, 0.015	$gCd^{-1}(Wm^{-2})^{-1}$	Based on ranges found in (Platt et al. 1980) and tuned separately for each lake region (South, North)

Parameter	Abbreviation	Value	Units	Source
Sediment respiration flux	r_{SED}	0.05 – 0.4	$g\ m^{-2} day^{-1}$	Based on ranges found in (Ladwig et al. 2021) and (Mi et al. 2020) and fit independently for each lake
Respiration rate of DOCL	r_{DOCL}	0.015 – 0.025	day^{-1}	Based on ranges found in (McCullough et al. 2018) and fit for each lake independently

339

340   **2.3.4 Internal Lake Metabolism Fluxes**

341   The metabolism fluxes in the model are net primary production (NPP) and respiration (R).

342   Respiration includes water column respiration for each OC state variable in the epilimnion

343   and hypolimnion and is calculated at each time step as the product of the OC state variable

344   and its associated first order decay rate (Table 2, Eq. 13). Sediment respiration for the

345   hypolimnion during stratified periods and the epilimnion (entire lake) during mixed periods

346   is a constant daily rate that is individually fit for each lake. Note that we did not include

347   anaerobic carbon metabolism in our modeling approach and discuss potential shortcomings

348   in the discussion section. We assume inorganic carbon is not a limiting carbon source. In the

349   model, we consider any DO concentration less than 1 g DO m^{-3} to be anoxic (Nürnberg

350   1995).

351

352   NPP is tracked in both the epilimnion and hypolimnion. NPP is a function of light, total

353   phosphorus concentration, temperature, a maximum productivity coefficient (*Pmax*), and a

354   slope parameter defining the irradiance and productivity curve (*IP*) (Table 2 Eq. 12). Total

355   phosphorus concentration in a layer ~~taken is from~~ is taken from observational data for each

356   lake interpolated to the daily time scale. Maximum daily primary production rates were taken

19

357 from Wetzel (2001). As these maximum production rates are not phosphorus-specific but

358 subsume lake-specific nutrient concentrations, we multiplied them with time-transient,

359 normalized TP concentrations. Normalizing was done by removing the mean of observed TP

360 and dividing by TP variance. This allows us to retain the time dynamics of the normalized

361 TP, which we use to represent seasonal TP dynamics for each lake. The Arrhenius equation

362 provides temperature control for NPP, and we determined through model fitting a θ of 1.12.

363 All OC derived from NPP is assumed to be labile and is split between particulate and

364 dissolved OC production, with eighty percent produced as POC and twenty percent produced

365 as DOC. This ratio was determined through model fitting and is similar to previously

366 reported values (Hipsey et al. 2022). Average light in a layer is calculated for each day and is

367 dependent on the depth of a layer and the light extinction coefficient (Table 2 Eq. 19). During

368 ice covered conditions, average light is assumed to be five percent of the average non-ice

369 covered value (Lei et al. 2011).

370

371 Epilimnetic and hypolimnetic water column respiration is tracked independently for each OC

372 pool in the model. During mixed periods, there are four OC pools – DOCR, DOCL, POCR,

373 POCL. During stratified periods, those pools are split into a total of eight pools that are

374 tracked independently for the epilimnion and hypolimnion. Respiration is calculated as a

375 product of the mass of a respective variable, a first order decay rate coefficient, temperature,

376 and oxygen availability (Table 2 Eq. 13). The respiration decay rate coefficients are based on

377 literature values (Table 3) or were fit during model calibration. An Arrhenius equation is

378 used for temperature control of respiration, with θ_{Resp} equal to 1.04, which was determined

20

379   through manual model fitting. The respiration fluxes are also scaled by oxygen availability

380   using the Michaelis-Menten equation with a half saturation coefficient of 0.5 g DO m^{-3}, such

381   that at very low DO concentrations, the respiration flux approaches zero.

382

383   Sediment respiration is calculated from a constant daily respiration flux, adjusted for

384   temperature and oxygen availability, using the Arrhenius and Michaelis-Menten equations,

385   respectively (Table 2 Eq. 14). The mass of sediment OC is not tracked in the model. During

386   stratified periods, we assume that the majority of epilimnetic sediment area is in the photic

387   zone, and therefore has associated productivity from macrophytes and other biomass. It is

388   assumed that this background productivity and sediment respiration are of similar magnitude

389   and inseparable from water column metabolism, given the observational data. Therefore,

390   epilimnetic sediment respiration is not accounted for in the model during stratified

391   conditions. During mixed conditions, we assume that sediment respiration is active on all

392   lake sediment surfaces, which are assumed to be equivalent in area to the total surface lake

393   area. During stratified periods, we use the area at the thermocline as the sediment area for

394   calculating hypolimnetic sediment respiration.

395

396   **2.3.5 Other in-lake calculations and assumptions**

397   We calculate a total light extinction coefficient (LEC) for the epilimnion and hypolimnion.

398   The total LEC for each layer is calculated by multiplying the dissolved and particulate

399   specific LEC values with their respective OC state variable concentrations, combined with a

400   general LEC value for water (Table 2 Eq. 20). This total LEC value is used to calculate a

21

401   daily estimate of Secchi depth (Table 2 Eq. 8). The coefficients for the light extinction of

402   water, DOC, and POC are manually calibrated based on observed Secchi depth ranges for the

403   study lakes (Table 3, SI Table 5).

404

405   **Table 3.** Model Parameters, grouped into three categories: constants, which are values that
406   were not tuned; manually calibrated, which are parameters manually tuned, typically guided
407   by ranges from the literature; and parameters calibrated through constrained parameter
408   search, which are calibrated through an automated search of parameter space.
409

Parameter	Abbreviation	Value	Units	Source
Constants				
Conversion of Carbon to Oxygen	$O2_{convert}$	2.67	Unitless	Mass Ratio of C:O
Respiration rate of DOCR	r_{DOCR}	0.001	day^{-1}	(Hanson et al., 2011)
Respiration rate of POCR	r_{POCR}	0.005	day^{-1}	Taken from ranges provided in (Hanson et al. 2004)
~~Respiration rate of POCR~~	~~r_{POCR}~~	~~0.005~~	~~day^{-1}~~	~~Taken from ranges provided in (Hanson et al. 2004)~~
Respiration rate of POCL	r_{POCL}	0.2	day^{-1}	Taken from ranges provided in (Hipsey et al. 2022)
Michaelis-Menten DO half saturation coefficient	$DO_{1/2}$	0.5	$g\ m^{-3}$	Taken from ranges provided in (Hipsey et al. 2022)
Light extinction coefficent of water	LEC_{water}	0.125	m^{-1}	Taken from ranges in Hart et al. (2017)
Ratio of DOC to POC production from NPP	C_{NPP}	0.8	Unitless	Biddanda & Benner (1997)
Albedo	α	0.3	Unitless	Global average (Marshall & Plumb, 2008)
Atmospheric gas exchange adjustment during ice covered conditions	C_{winter}	0.1	Unitless	Taken from ranges in (Loose & Schlosser, 2011)

22

Parameter	Abbreviation	Value	Units	Source
Coefficient of light transmitted through ice	C_{ice}	0.05	Unitless	Taken from ranges provided in (Lei et al. 2011)
Settling velocity rate of POC_R	K_{POCR}	1.2	$m\ day^{-1}$	Taken from ranges found in (Reynolds et al.1987)
Settling velocity rate of POC_L	K_{POCL}	1	$m\ day^{-1}$	Taken from ranges ranges found in (Reynolds et al.1987)
Temperature scaling coefficient for NPP	θ_{NPP}	1.12	Unitless	Taken from values provided in (Hipsey et al. 2022) and (Ladwig et al. ~~2022~~ 2021)
Temperature scaling coefficient for Respiration	θ_{Resp}	1.04	Unitless	Taken from values provided in (Hipsey et al. 2022) and (Ladwig et al. ~~2022~~ 2021)
Manually calibrated				
Light extinction of DOC	LEC_{DOC}	0.02 - 0.06	$m^2 g^{-1}$	Manually calibrated based on observed Secchi Depth ranges for the study lakes
Light extinction of POC	LEC_{POC}	0.7	$m^2 g^{-1}$	Manually calibrated based on observed Secchi Depth ranges for the study lakes
Maximum Daily Productivity	$Pmax$	0.5-5	$g\ m^{-3} day^{-1}$	Manually calibrated from mean productivity values from Wetzel (2001)
Recalcitrant DOC inflow concentration	$DOCR_{inflow}$	5-10	$g\ m^{-3}$	Based on ranges found in (Hanson et al. 2014, McCullough et al. 2018, Hart et al. 2017)
Recalcitrant POC inflow concentration	$POCR_{inflow}$	2-5	$g\ m^{-3}$	Based on ranges found in (Hanson et al. 2014, McCullough et al. 2018, Hart et al. 2017)
Calibrated through constrained parameter search				

Parameter	Abbreviation	Value	Units	Source
Slope of the irradiance/productivity curve	IP	0.045, 0.015	$gCd^{-1}(Wm^{-2})^{-1}$	Based on ranges found in (Platt et al. 1980) and tuned separately for each lake region (South, North)
Sediment respiration flux	r_{SED}	0.05 – 0.4	$g\ m^{-2}day^{-1}$	Based on ranges found in (Ladwig et al. 2021) and (Mi et al. 2020) and fit independently for each lake
Respiration rate of DOCL	r_{DOCL}	0.015 - 0.025	day^{-1}	Based on ranges found in (McCullough et al. 2018) and fit for each lake independently

410

2.4 Model Sensitivity and Parameter Calibration

To better understand the sensitivities of the model output to parameter values, we performed

a sensitivity analysis of the model parameters using the global sensitivity method from

Morris (1991). The sensitivity analysis showed that there were nine parameters to which the

model was consistently sensitive across the six study lakes. This group included the ratio of

DOC to POC produced from NPP (C_{NPP}), the maximum daily productivity parameter

(*Pmax*), the inflow concentration of recalcitrant POC ($POCR_{inflow}$), the setting velocity of

recalcitrant POC (K_{POCR}), the temperature fitting coefficients for productivity and respiration

(θ_{NPP}, θ_{Resp}) the slope of the irradiance/productivity curve (*IP*), the sediment respiration flux

(r_{SED}), and the respiration rate of DOCL (r_{DOCL}). We chose a subset of the nine parameters to

include in the uncertainty analysis based on the following justifications. The model results

showed that recalcitrant substrates are of lesser importance for lake metabolism dynamics, so

we chose not to further investigate the uncertainty of the $POCR_{inflow}$ and K_{POCR} parameters.

The *Pmax* and *IP* parameters are directly correlated, so we chose to remove Pmax from

24

425   further uncertainty considerations. The θ_{NPP} and θ_{RESP} parameters act as substitutes for water

426   temperature, a well-known "master variable" in water quality modeling, and directly reflect

427   seasonality in the model. Therefore, we chose to omit these parameters for further

428   uncertainty calculations. The final subset of parameters for uncertainty analysis consisted of

429   C_{NPP}, r_{DOCL}, r_{SED}, and IP. Of the four parameters, we felt C_{NPP} was best constrained by the

430   literature. To reduce the number of parameters estimated in the calibration process we

431   restricted the automated constrained parameter search to the remaining three.

432
433   Model parameters are grouped into three categories: constants, manually calibrated, and

434   parameters calibrated through an automated constrained parameter search. The constant

435   parameters are consistent across the study lakes and are not tuned. The manually calibrated

436   parameters were allowed to vary by lake and are typically guided by ranges from the

437   literature. The constrained parameter search uses an automated search of parameter space,

438   constrained by literature values, to fit the IP, r_{SED}, and r_{DOCL} parameters for the study lakes.

439   Specifically, we performed a constrained fitting of the model to observational data using the

440   Levenberg-Marquardt algorithm within the "modFit" function of the "FME" R package

441   (Soetaert & Petzoldt, 2010). During the model fitting, errors in modeled DO, DOC, and

442   Secchi depth are weighted equally in the southern lakes. Secchi depths in the northern lakes

443   were highly stochastic, and therefore we use a moving average on observational data and

444   predictions of Secchi depth and calculate the residuals as the difference between the two

445   averaged time series. We use a moving average window of 15 observations because we want

446   to capture the average annual Secchi depth trend, and there are roughly 15 observations per

447   year.

25

448

449   The first 15 years of the model output was used for calibration and the last 5 years were used

450   for model validation. We chose the first 15 years for calibration because the observational

451   data were relatively stable and were not indicative of any large trends in ecosystem

452   processes, as opposed to the last five years which showed slightly more model deviation

453   from DOC observational data in the southern lakes (SI Fig. 2).

454

455   **2.5 Model Uncertainty**

456   Sensitivity guided the uncertainty analysis. To quantify uncertainty around model

457   predictions, we sampled IP, r_{SED}, and r_{DOCL} simultaneously from uniform distributions

458   defined by +-30% of the literature ranges used for our calibrated parameter values (Table 3).

459   We ran one hundred model iterations randomly sampling the three model state variables

460   across these distributions. We plotted the minimum and maximum values for these uniform

461   distributions and included them in the time series plots (Fig. 2, 3, 4, SI Fig. 1,2,3).

462

463   **3 Results**

464
465   **3.1 Model Fit to Ecosystem States**

466   Model predictions of DO reproduce observed seasonal variability well. Note that RMSE

467   values presented here represent model error combined over both the validation and

468   calibration periods (see Supplementary Material: Table S1 for calibration and validation

469   specific RMSE values), and that state variables are presented with truncated time ranges for

470   visual clarity (see Supplementary Material: Fig. S1-S3 for full time series). Epilimnetic DO

26

471   generally has lower RMSE than DO in the hypolimnion (Fig. 2). In the epilimnion, RMSE

472   ranges from 0.74 g DO m^{-3} (TR) to 2.11 g DO m^{-3} (MO), and in the hypolimnion, RMSE

473   ranges from 1.22 g DO m^{-3} (ME) to 2.77 g DO m^{-3} (AL, SP). Validation NSE values for DO

474   ranged from -1.45 (AL) to 0.02 (ME) in the epilimnion and -0.30 (SP) to 0.86 (ME) in the

475   hypolimnion. Validation KGE values for DO ranged from 0.40 (AL) to 0.90 (TR) in the

476   epilimnion and 0.35 (SP) to 0.80 (ME) in the hypolimnion. KGE and NSE values for all

477   lakes can be found in SI Table 7. In the southern lakes, modeled values reach anoxic levels

478   and generally follow the DO patterns recorded in the observed data (Fig. 2a-b).

479   Observational data for the northern lakes show an occasional late summer onset of anoxia,

480   and these events are generally captured in the model output. A late summer spike in

481   hypolimnetic DO predictions commonly occurs as well, which is likely a model artifact

482   caused by the reduction of hypolimnetic volumes to very small values over short time periods

483   prior to fall mixing. Reduction to small volumes, coincident with modest fluxes due to high

484   concentration gradients, result in transient high concentrations. Overall, the goodness-of-fit

485   of hypolimnetic DO in our study lakes does not seem to follow any regional or lake
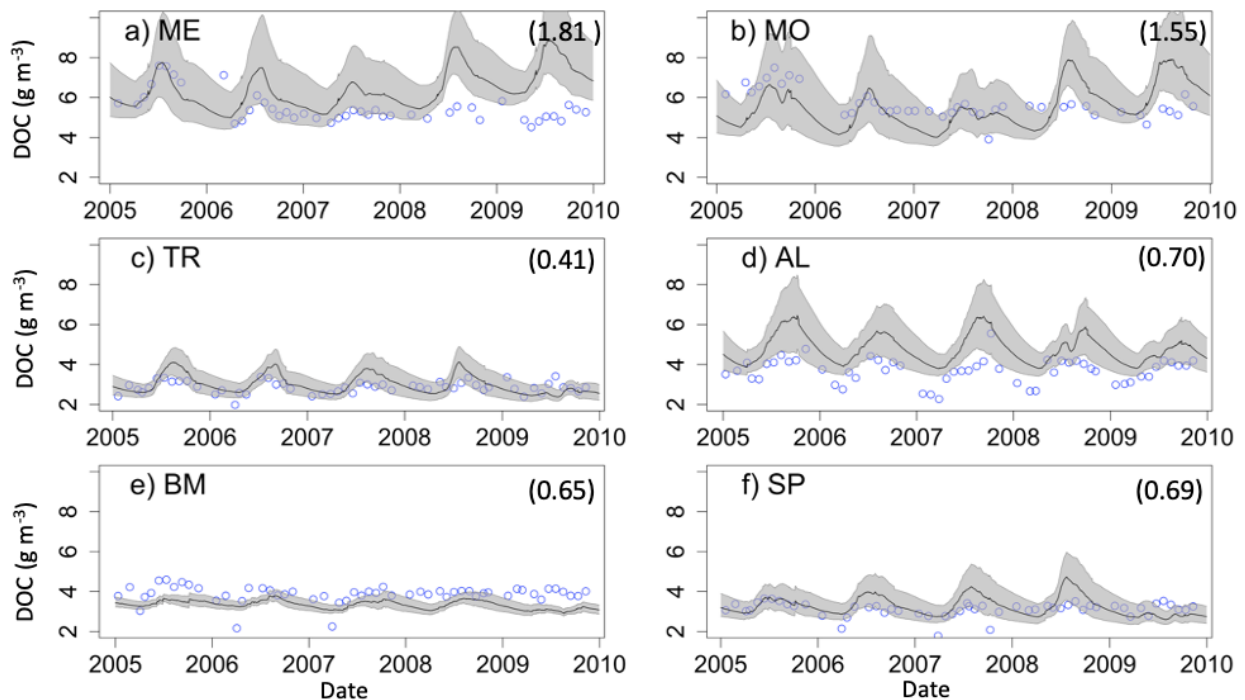
486   characteristic patterns.

27
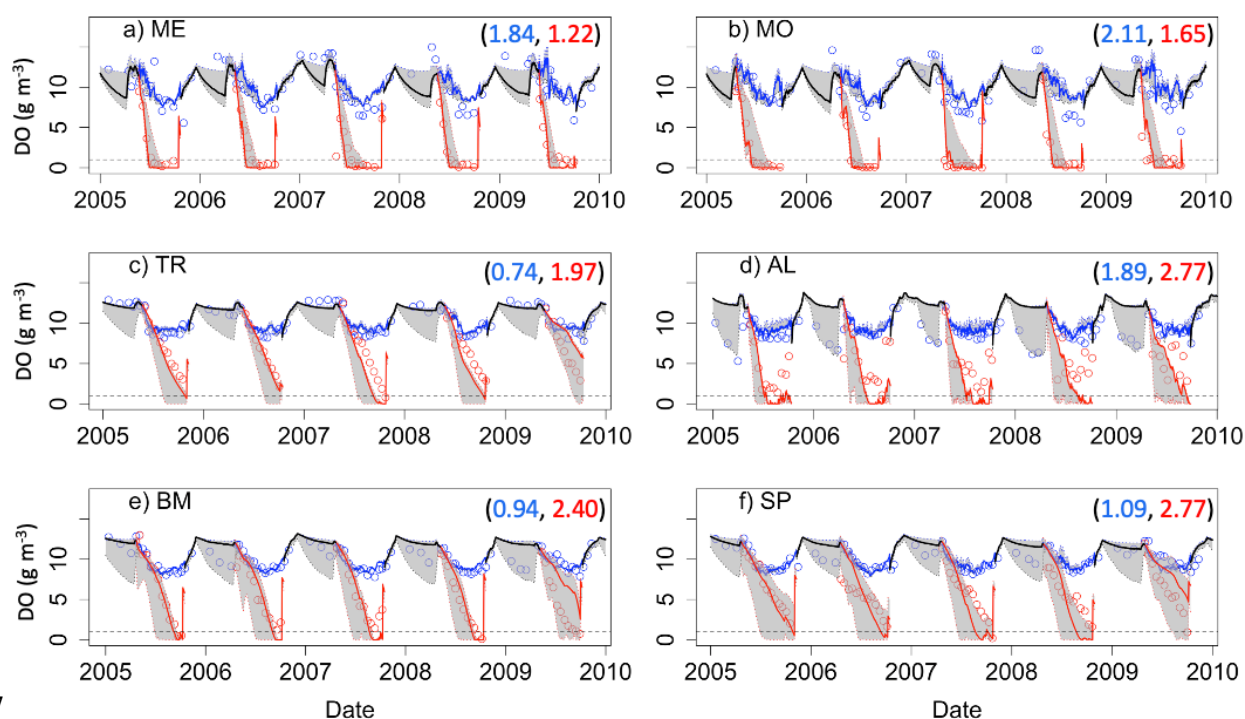
Figure 2. Dissolved oxygen (DO) time series for the years, 2005-2010, for the six study lakes (a-f). Model predictions are represented by lines, and circles represent the observational data. Epilimnetic DO values are blue and Hypolimnetic DO values are red. Fully mixed periods for the lake are indicated by a single black line. RMSE values (epilimnion, hypolimnion; $g\ m^{-3}$) for the validation period are included in the upper right of each panel. Uncertainty is represented by gray shading.

The two southern lakes (ME, MO) have epilimnetic DOC RMSE values greater than 1.00 g C m^{-3}, while the RMSE for northern lakes ranges from 0.41 g C m^{-3} (TR) to 0.70 g C m^{-3} (AL) (Fig. 3). In the southern lakes, NSE epilimnetic DOC values were below -3.00 and KGE values ranged from -0.29 to -0.32. In the northern lakes, NSE values for DOC ranged between -2.75 (SP) and -0.31 (AL). KGE values ranged from -0.07 (BM) to 0.35 (TR). All NSE and KGE metrics for DOC can be found in SI Table 7. Observational data in both southern lakes indicate a decrease in DOC concentration beginning around 2010, which is largely missed in the model predictions (Fig.3a-b, Supplementary Material: Fig. S2a-b) and

28

504 cause an overestimation of DOC by about 1-2 g C m^{-3}. However, model predictions converge

505 with observed DOC toward the end of the study period (Supplementary Material: Fig. S2a-

506 b). In AL, the seasonal patterns of modeled DOC are smaller in amplitude than the

507 observational data (Supplementary Material: Fig. S2d).

508

509
510 **Figure 3.** Epilimnetic dissolved organic carbon (DOC) time series for the years, 2005-2010,
511 for the six study lakes (a-f). Model predictions are represented by lines, and circles represent
512 the observational data. RMSE values for the validation period are included for each lake (g C
513 m^{-3}). Uncertainty is represented by gray shading.
514

515 Secchi depth predictions reproduce the mean and seasonal patterns in all lakes (Fig. 4).

516 Although the model produced annual cycles of Secchi depth that generally covered the range

517 of observed values, short term deviations from annual patterns in the observed data are not

518 reproduced. The timing of minima and maxima Secchi depth sometimes differed between

519 predicted and observed values for the northern lakes. In addition, winter extremes in

29

520 observed Secchi depth are not always reproduced by the model, which is especially evident

521 for ME (Fig. 4a). However, winter observational data for Secchi are more sparse than other

522 seasons.

523
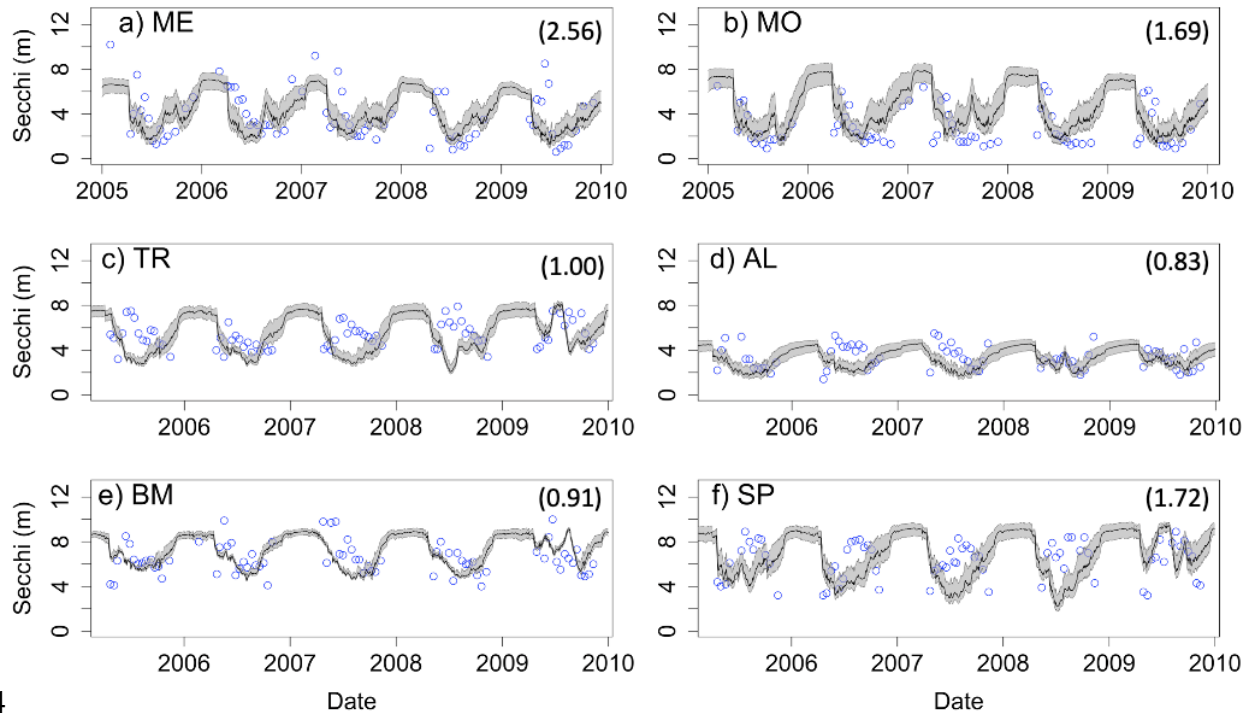
524
525 **Figure 4.** Secchi depth time series for the years, 2005-2010, for the six study lakes (a-f).
526 Model predictions are represented by lines, and circles represent the observational data.
527 RMSE values for the validation period are included for each lake (m). Uncertainty is
528 represented by gray shading.
529

530 **3.2 Ecosystem Processes**

531 The mean annual OC budgets of all six lakes show large differences in the sources and fates

532 of OC among lakes (Fig. 5; Supplementary Material: Table S3). Autochthony is the dominant

533 source of OC for all study lakes. Water column respiration is the largest portion of whole-

534 lake respiration in ME, MO, TR, SP, and BM. Sediment respiration contributions are a lower

535 proportion of total respiration in ME, MO, and TR (mean of 14.1%), and are slightly higher

30

536   in BM and SP (mean of 18.7%). AL has a more even distribution of OC fates. OC burial

537   amounts also vary across the study lakes, with the highest percentage in AL (34.1%), and

538   lowest in SP (5.25%).

539
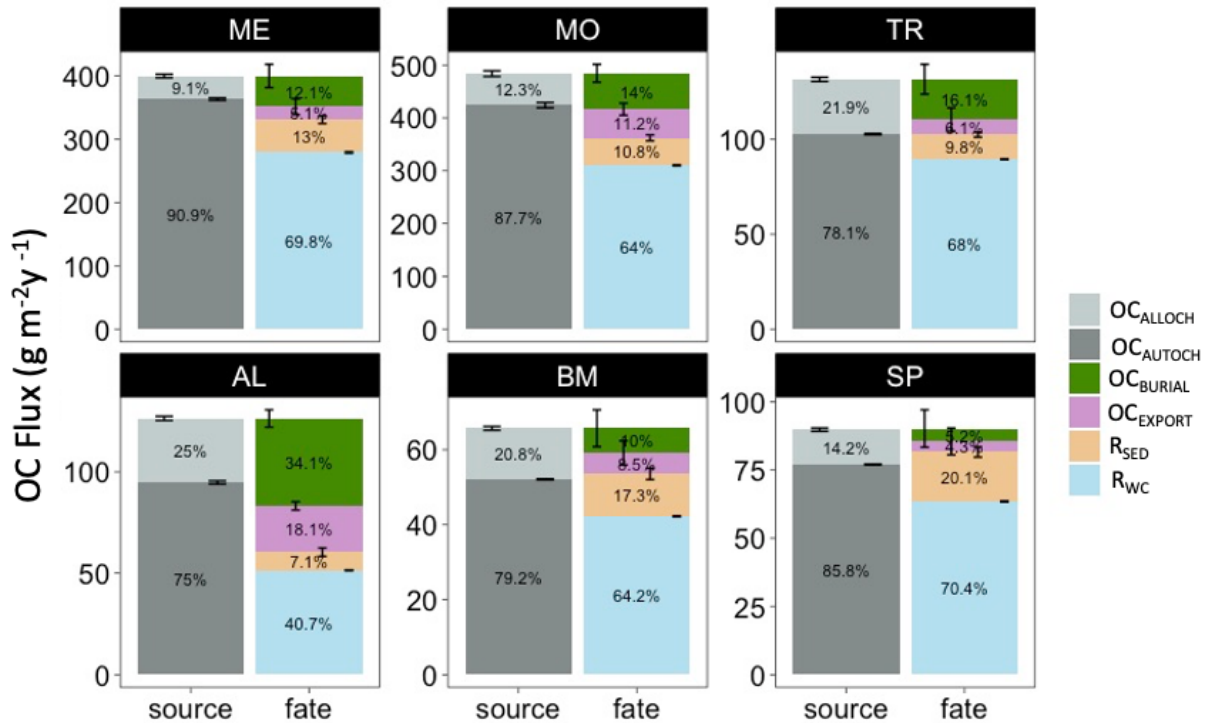
540
541 **Figure 5.** Total annual budget, sources (left stacked bars) and fates (right stacked bars), of
542 organic carbon (OC) in each lake over the study period. The OC sources include
543 allochthonous OC (OC_{ALLOCH}) and autochthonous OC (OC_{AUTOCH}). The OC fates include
544 burial of OC (OC_{BURIAL}), export of OC (OC_{EXPORT}), sediment respiration of OC (R_{SED}), and
545 water column respiration of OC (R_{WC}). Standard error bars for the annual means are
546 indicated for each source and fate as well. Note that the magnitudes of the y-axis differ
547 among the lakes. A significance test comparing these fluxes across the study lakes can be
548 found in SI Table 6.

549

550   The lakes show inter-annual variation in trophic state, as quantified by NEP (Fig. 6). Total

551   respiration (water column and sediment) exceeds autochthony in SP, BM, and TR, indicating

552   predominantly net heterotrophy for these systems. The remaining lakes (ME, MO, AL) are

31

553   generally net autotrophic. The southern lakes (ME, MO) are net autotrophic (positive NEP)

554   for the majority of the study years but became less autotrophic over the last five years of the

555   study period (2010-2014). BM and SP are mostly net heterotrophic (negative NEP) over the

556   study period with a few brief instances of net autotrophy. The strongest autotrophic signal for

557   these lakes occurred around 2010. TR experienced prolonged periods of both autotrophy and

558   heterotrophy. AL is net autotrophic over the study period but had lower average NEP than

559   the southern lakes. ME, MO, and AL all have negative trends in NPP, but only ME and AL

560   were significant (p_value < 0.1, Mann-Kendall test) (SI Table 2). Of these three lakes, ME

561   and AL also have decreasing significant trends in annual total phosphorus concentration (SI

562   Table 2). No significant trends were found for NPP or total phosphorus in the other lakes

563   (MO, TR, BM, SP). It is worth noting that our interpretation of metabolism dynamics in

564   the results are based on the median NPP and Respiration flux values produced by the model.

565   Because of the high uncertainty associated with these fluxes, we should be cautious about

566   asserting inferences about long term changes in trophic state.
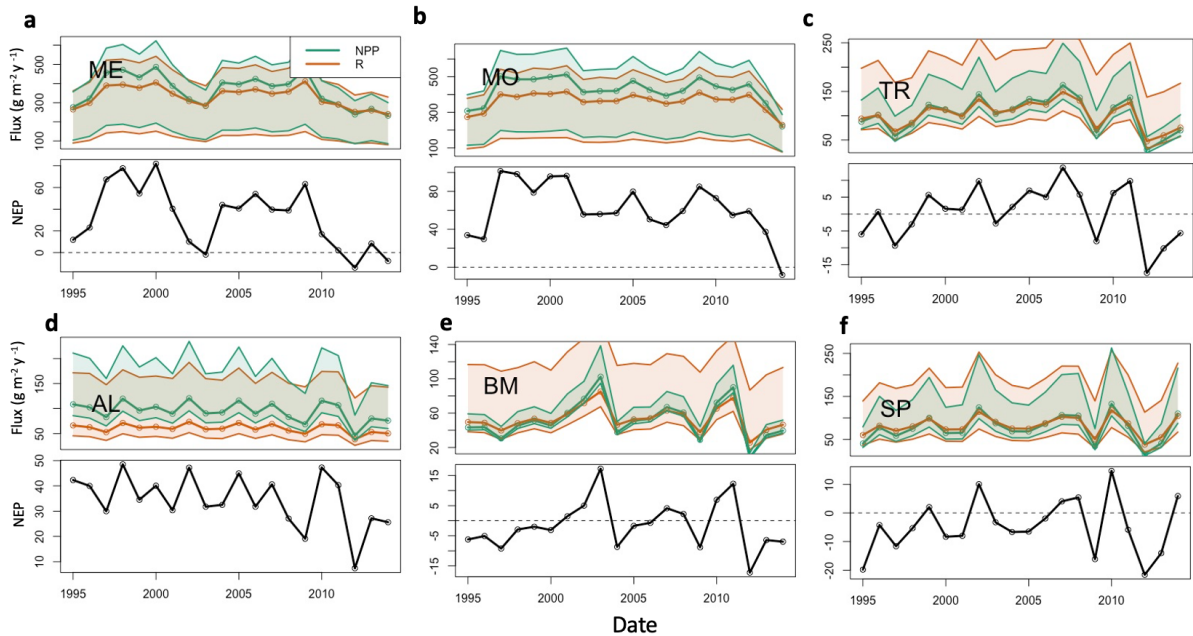
Figure 6. Time series of calibrated lake Net Primary Production (green), Total Respiration (red) (top panels), and Net Ecosystem Production (NEP, bottom panels) for the six lakes: (a) Lake Mendota; (b) Lake Monona; (c) Trout Lake; (d) Allequash Lake; (e) Big Muskellunge Lake, and; (f) Sparkling Lake. Fluxes are in units of $gC\ m^{-2}y^{-1}$. Solid line represents prediction based on best parameter estimates. Shaded regions represent prediction uncertainty based on parameter ranges in Table 3. Shaded region for NEP not shown to reduce axis limits and emphasize NEP pattern.

Hypolimnetic DO consumption during stratified periods was modeled as a function of the

two components of hypolimnetic respiration, hypolimnetic water column respiration and

hypolimnetic sediment respiration. Water column respiration contributes more than sediment

respiration to total hypolimnetic respiration ~~in the southern lakes compared to the northern~~

~~lakes, with the exception of TR, where cumulative water column respiration is much larger~~

~~than cumulative sediment respiration~~ in the deepest lakes. In ME and MO, the mass of

summer autochthonous POC entering the hypolimnion is similar to the total hypolimnetic OC

mass respired for the beginning of the stratified period (Fig. 7a-b; green line). Later in the

stratified period, an increase in epilimnetic POC and associated settling exceeds total

33

586 hypolimnetic respiration (Fig. 7a-b; green hashed area). This is due, in part, to lower

587 respiration rates that occur once DO (gray line) has been fully depleted, which occurs in early

588 July for ME and late June for MO. In BM and SP the total hypolimnetic respiration slightly

589 exceeds autochthonous POC inputs during parts of the stratified period, indicating the

590 importance of allochthony in these systems (Fig. 7c,f). BM shows that autochthonous POC

591 entering the hypolimnion and total hypolimnetic respiration are similar for much of the

592 stratified period (Fig. 7d). AL is the only lake to have autochthonous POC inputs consistently

593 larger than total hypolimnetic respiration during the stratified season. All lakes show that

594 summer allochthonous POC entering the hypolimnion is a small contribution to the overall

595 hypolimnetic POC load.

596
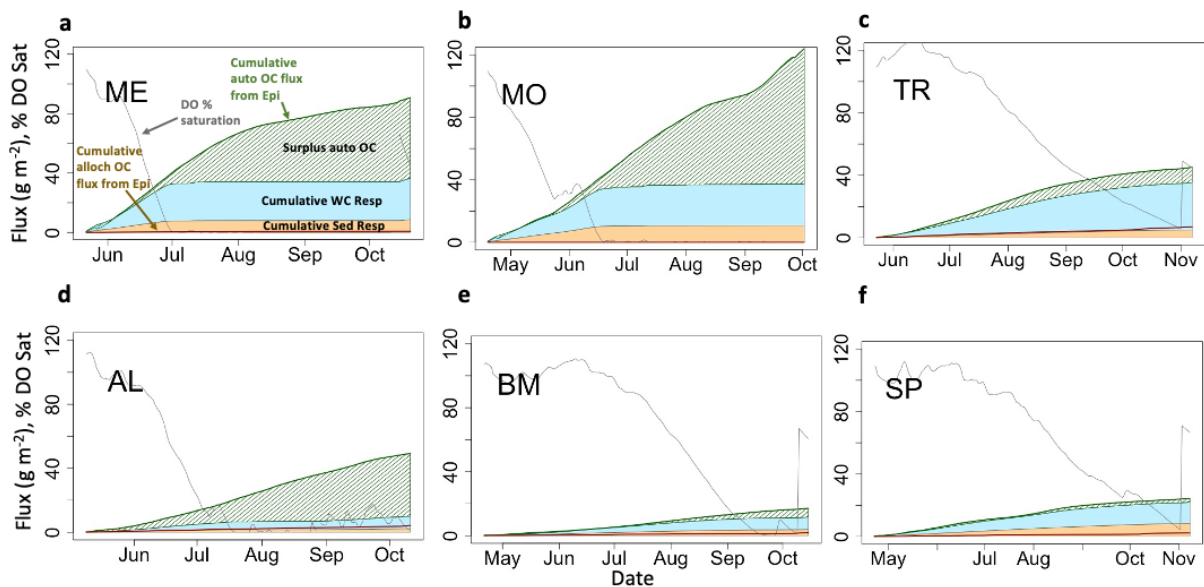
597
598 **Figure 7.** Hypolimnetic dissolved oxygen, allochthonous (alloch) and autochthonous (auto)
599 organic carbon loading, and respiration dynamics during one stratified period (2005) for each
600 lake. Fluxes are cumulative $gC\ m^{-2}$ and DO is presented as percent saturation. Labels are in
601 panel (a). Note that the cumulative water column (WC) and sediment (Sed) respiration fluxes
602 are stacked, while other cumulative fluxes are not.

603

34

604 Respiration of autochthonous POC and sediment respiration account for most of the total

605 hypolimnetic respiration in all lakes (Fig. 8). Respiration of DOC accounts for a relatively

606 small proportion of total respiration. Total hypolimnetic respiration is higher in the southern

607 lakes than the northern lakes. TR has the highest amount of hypolimnetic respiration for the

608 northern lakes, and AL and BM have the least amounts of hypolimnetic respiration. Water

609 column respiration contributed the most towards total hypolimnetic respiration in all lakes.

610 Sediment respiration contributed the largest proportion towards total hypolimnetic respiration

611 in BM and SP. DOC water column respiration was the smallest proportion of total

612 hypolimnetic respiration in all six study lakes.
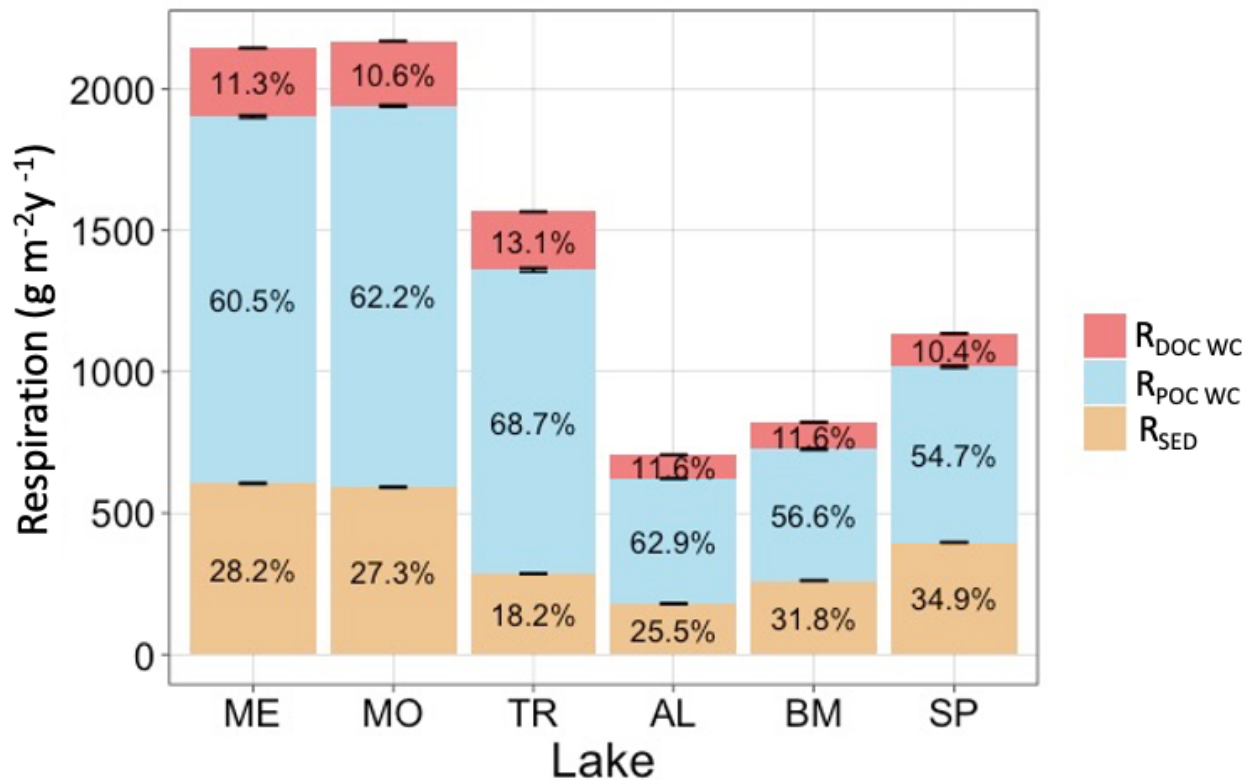
613
614 **Figure 8.** Total average annual hypolimnetic respiration, separated by percentages attributed
615 to water column DOC ($R_{DOC\,WC}$), water column POC ($R_{POC\,WC}$), and sediment (R_{SED}) organic
616 carbon sources. Standard error bars for the annual respiration values are indicated as well.
617

35

4 Discussion

4.1 Autochthonous and Allochthonous Loads

~~Autochthony was the dominant source of OC subsidizing hypolimnetic respiration in the study lakes. The importance of autochthonous OC pools in ecosystem respiration was surprising, given ample research highlighting the dominance of allochthonous OC in north temperate lakes (Wilkinson et al. 2013; Hanson et al. 2011; Hanson et al. 2014). This outcome emphasizes the utility of process-based models in studying mechanisms that discern the relative contributions of different pools of organic matter to lake metabolism. Autochthonous OC pools have higher turnover rates than allochthonous OC pools (Dordoni et al., 2022) and often are lower in concentration than the more recalcitrant allochthonous pools (Wilkinson et al. 2013).~~ Autochthony was the dominant source of OC subsidizing hypolimnetic respiration in the modeling results for our study lakes. The high contribution of autochthonous OC to ecosystem respiration, relative to that of the allochthonous pool, was surprising, given ample research highlighting the dominance of allochthonous OC in north temperate lakes (Wilkinson et al. 2013; Hanson et al. 2011; Hanson et al. 2014). Similar to what was found by Wilkinson et al (2013), the standing stock of DOC in the water column of lakes in our study was from predominantly allochthonous sources. However, we emphasize in our study that autochthonous OC pools have higher turnover rates than allochthonous OC pools (Dordoni et al., 2022) and often are lower in concentration than the more recalcitrant allochthonous pools (Wilkinson et al. 2013). Thus, studies based on correlative relationships between lake concentrations of organic matter and water quality metrics, likely overlook the

36

640   importance of more labile organic matter in driving observable ecosystem phenomena, such

641   as gas flux and formation of hypolimnetic anoxia (Evans et al., 2005; Feng et al., 2022). By

642   quantifying metabolism fluxes relevant to both OC pools, we can recreate shorter-term OC

643   processes that quantify high turnover of labile organic matter, which would typically be

644   missed by empirical studies based on monthly or annual observations.

645

646   Allochthony and autochthony are important to lake carbon cycling, but in ways that play out

647   at different time scales. Allochthonous OC has been well-established as an important factor

648   in driving negative NEP through a number of mechanisms (Wilkinson et al., 2013; Hanson et

649   al., 2014; Hanson et al., 2011). Allochthony contributes to water quality variables, such as

650   Secchi depth (Solomon et al. 2015), by providing the bulk of DOC in most lakes (Wilkinson

651   et al., 2013) and can drive persistent hypolimnetic anoxia in dystrophic lakes (Knoll et al.,

652   2018). In contrast, autochthony contributes to seasonal dynamics of water quality through

653   rapid changes in OC that can appear and disappear within a season. Within that seasonal time

654   frame, autochthonous POC settling from the epilimnion can drive hypolimnetic respiration,

655   thus controlling another key water quality metric, oxygen depletion. It is worth noting that

656   our model does not discern allochthonous and autochthonous sediment OC, however we

657   show that autochthonous OC makes up the largest proportion of OC loads in our study lakes

658   and therefore autochthony likely contributes substantially to the sediment OC pool. For

659   highly eutrophic lakes, the model results show excess autochthony stored in the sediments

660   which may carry into subsequent years, potentially providing additional substrate for

37

661   sediment respiration. Thus, understanding and predicting controls over hypolimnetic oxygen

662   depletion benefits from quantifying both allochthonous and autochthonous OC cycles.

663

664   Differences in trophic status, hydrologic residence time, and inflow sources help explain the

665   relative proportion of allochthonous versus autochthonous OC among lakes in our study.

666   Water residence times (Hotchkiss et al. 2018; McCullough et al. 2018) and surrounding land

667   cover (Hanson et al. 2014) have been shown to have a substantial impact on OC dynamics by

668   controlling allochthonous OC loading and NEP trends on lakes included in our study

669   (Hanson et al. 2014, McCullough et al. 2018). We built upon these ideas by recreating daily

670   watershed loading dynamics of POC and DOC from derived discharge data and incorporating

671   nutrient control over lake primary production by using high quality and long-term

672   observational data. The northern lakes are embedded in a forest and wetland landscape,

673   which are characteristic of having higher DOC than the urban and agricultural landscape of

674   the southern lakes (Creed et al., 2003). This creates variation in allochthonous loading across

675   the study lakes. Lake trophic state and productivity are a major control for autochthonous

676   production, which influences autochthonous loads across the study lakes as well. For lake

677   metrics that are comparable between studies, such as allochthonous loading and export,

678   allochthonous water column respiration, and total OC burial, our results were within 20% of

679   values in related studies (Hanson et al. 2014, McCullough et al. 2018).

680

681   **4.2 Hypolimnetic Respiration**

38

682 Given the importance of autochthonous POC to hypolimnetic respiration, we assume it

683 contributes substantially to both sediment respiration and respiration in the water column.

684 While previous work found that sediment respiration was the dominant respiration source for

685 lakes with depth ranges encompassed within our study (Steinsberger 2020), we found that

686 water column respiration was at least as important, if not more so. Differences in these

687 findings could be linked to uncertainty in the settling velocity of POC, due to lack of

688 empirical POC settling velocity measurements. Perhaps, POC mineralized in the hypolimnia

689 of our modeled lakes passes more quickly to the sediments in real ecosystems, shifting the

690 balance of respiration more toward the sediments. OC respiration can contribute substantially

691 to hypolimnetic DO depletion in both lakes and reservoirs (Beutel, 2003), and POC settling

692 velocities can be highly variable, suggesting that assumptions around vertical distribution of

693 lake POC deserve further investigation. Another possible explanation for these differences

694 could be that our model missed allochthonous POC loads from extreme events (Carpenter et

695 al., 2012), which can increase the amount of legacy OC stored in the sediments and increase

696 sediment respiration. Our model also does not account for reduced respiration rates due to

697 OC aging, which may explain our higher values of water column respiration. Finally, our

698 model includes entrainment as a possible oxygen source to the hypolimnion, which must be

699 offset by respiration to fit observed hypolimnetic DO changes. Any study that underestimates

700 DO sources to the hypolimnion likely underestimates total respiration.

701

702 Anaerobic mineralization of organic carbon is an important biogeochemical process and can

703 be a substantial carbon sink through methanogenesis (Maerki et al. 2009). Although

39

704   methanogenesis is not incorporated into our model, methane dissolved in the water column of

705   Lake Mendota is mostly oxidized (Hart 2017), thus contributing to the overall oxygen

706   demand, which is accounted for in our model. What remains unaccounted is ebullition of

707   methane, which is a carbon flux that is difficult to quantify (McClure et al. 2020). Future

708   metabolism studies that include these processes might find a decrease in annual OC burial

709   rates relative to rates in our study. Although we believe that ebullition is not a substantial

710   portion of the lake's carbon mass budget, that remains to be studied more carefully. As the

711   model accounts for DO consumption through calibration, the overall flux would not change

712   even if we link DO consumption to methane oxidation, only the process description would be

713   more realistic.

714

715   Our findings highlight the importance of autochthonous POC in hypolimnetic oxygen

716   depletion and suggest that related processes, such as the timing of nutrient loading, changes

717   in thermocline depth, or zooplankton grazing, could impact overall lake respiration dynamics

718   and anoxia formation (Schindler et al., 2016; Ladwig et al., 2021; Müller et al., 2012). We

719   also recognize that the DO depletion rate in SP is more uncertain than in the other study

720   lakes. Although we are uncertain of the cause, we speculate that differences in morphometry

721   for this lake could impact the hypolimnetic volume and its capacity to hold DO as well as the

722   rate of sediment oxygen consumption (Livingstone & Imboden 1996). Although lake

723   hypsometry, along with thermal profile, controls the volume of hypolimnion in contact with

724   sediments in our model, there may be other factors related to morphometry (e.g., sediment

725   focusing) that remain unaccounted for, and we see this as an opportunity for future study.

726

4.3 Long-term Dynamics

Although autochthonous OC dominated the loads across the study lakes, analysis of the long-term OC dynamics supports the importance of allochthony in lakes. Net Ecosystem Production (NEP) has been used to quantify heterotrophy and autotrophy in lakes (Odum 1956, Hanson et al. 2003, Cole et al. 2000, Lovett et al. 2006), and using this metric over multiple decades allowed us to analyze long-term impacts of allochthony. TR, BM, and SP fluctuated between heterotrophy and autotrophy, usually in tandem with trends in hydrology, which acts as a main control of allochthonous OC. This suggests that allochthonous OC inputs may be less important for seasonal anoxia but can still drive a lake toward negative NEP and contribute to sediment carbon storage over long time periods. ME, MO, and AL tended to become less autotrophic over time (Fig. 6), a pattern that coincided with significant decreasing trends in mean epilimnetic total phosphorus concentrations for ME and AL (SI Fig. 5). In our model, NPP and phosphorus are directly related, so decreases in phosphorus are likely to cause decreases in NEP. Short-term respiration of autochthonous POC can account for rapid decreases in hypolimnetic DO, but allochthonous POC, which tends to be more recalcitrant, provides long-term subsidy of ecosystem respiration that can result in long-term net heterotrophy. Thus, it's critical to understand and quantify both the rapid internal cycling based on autochthony and the long and slow turnover of allochthony.

Through explicitly simulating the cycling of both allochthony and autochthony, we can expand our conceptual model of metabolism to better understand time dynamics of lake

41

748   water quality at the ecosystem scale. Autochthony has pronounced seasonal dynamics,

749   typically associated with the temporal variability of phytoplankton communities and the

750   growth and senescence of macrophytes (Rautio et al., 2011). While allochthony can also have

751   strong seasonal patterns associated with leaf litter input, pollen blooms, and spring runoff

752   events, its more recalcitrant nature leads to a less pronounced seasonal signal at the

753   ecosystem scale (Wilkinson et al., 2013, Tranvik 1998). When considered together, it seems

754   that allochthony underlies long and slow changes in metabolism patterns, while autochthony

755   overlays strong seasonality. Both OC pools are important for ecosystem scale metabolism

756   processes, and their consequences are evident at different time scales. Therefore, the

757   interactions of both OC sources and their influences on water quality patterns deserve further

758   investigation.

759

760   Autochthonous OC control over hypolimnetic respiration should be a primary consideration

761   for understanding the influence of OC on ecosystem dynamics. Hypolimnetic oxygen

762   depletion and anoxia in productive lakes can be mitigated by reducing autochthonous

763   production of OC, which we show is mainly driven by nutrient availability. This study also

764   identifies the need for a better understanding of internal and external OC loads in lakes.

765   Previous studies have found heterotrophic behavior in less productive lakes, but our findings

766   highlight the importance of autochthony in these lakes, especially for shorter-time scale

767   processes that can be missed by looking at broad annual patterns. By using a one-

768   dimensional, two-layer model, we are able to also understand how surface metabolism

769   processes can impact bottom layer dynamics, which would not be possible with a zero-

770   dimensional model. Looking forward, we believe that our understanding of these processes

771   could be improved by building a coupled watershed - metabolism model to more closely

772   explore causal relations between watershed hydrology, nutrient dynamics, and lake

773   morphometry.

774

775

776

777 *Code Availability*
778 Model code and figure creation code are archived in the Environmental Data Initiative
779 repository (https://doi.org/10.6073/PASTA/1B5B947999AA2F9E0E95C91782B36EE9,
780 Delany, 2022).
781
782 *Data Availability*
783 Driving data, model configuration files, and model result data are archived in the
784 Environmental Data Initiative repository
785 (https://doi.org/10.6073/PASTA/1B5B947999AA2F9E0E95C91782B36EE9, Delany, 2022).
786
787 *Author Contributions*
788 AD, PH, RL, and CB assisted with model development and analysis of results. AD and PH
789 prepared the manuscript with contributions from RL, CB, and EA.
790
791 *Competing Interests*
792 The authors declare that they have no conflict of interest.
793

804 <u>References</u>

805 Amon, R. M. W., & Benner, R. (1996). Photochemical and microbial consumption of

806   dissolved organic carbon and dissolved oxygen in the Amazon River system.

807   *Geochimica et Cosmochimica Acta*, *60*(10), 1783–1792. https://doi.org/10.1016/0016-

808   7037(96)00055-5

809 Beutel, M. W. (2003). Hypolimnetic Anoxia and Sediment Oxygen Demand in California

810   Drinking Water Reservoirs. *Lake and Reservoir Management*, *19*(3), 208–221.

811   https://doi.org/10.1080/07438140309354086

812 Bryant, L. D., Hsu-Kim, H., Gantzer, P. A., & Little, J. C. (2011). Solving the problem at the

813   source: Controlling Mn release at the sediment-water interface via hypolimnetic

814   oxygenation. *Water Research*, *45*(19), 6381–6392.

815   https://doi.org/10.1016/j.watres.2011.09.030

816 Cardille, J. A., Carpenter, S. R., Coe, M. T., Foley, J. A., Hanson, P. C., Turner, M. G., &

817   Vano, J. A. (2007). Carbon and water cycling in lake-rich landscapes: Landscape

818   connections, lake hydrology, and biogeochemistry. *Journal of Geophysical Research*,

819   *112*(G2), G02031. https://doi.org/10.1029/2006JG000200

820 Carpenter, S., Arrow, K., Barrett, S., Biggs, R., Brock, W., Crépin, A.-S., Engström, G.,

821   Folke, C., Hughes, T., Kautsky, N., Li, C.-Z., McCarney, G., Meng, K., Mäler, K.-G.,

822   Polasky, S., Scheffer, M., Shogren, J., Sterner, T., Vincent, J., … Zeeuw, A. (2012).

823   General Resilience to Cope with Extreme Events. *Sustainability*, *4*(12), 3248–3259.

824   https://doi.org/10.3390/su4123248

825 Carpenter, S. R., Benson, B. J., Biggs, R., Chipman, J. W., Foley, J. A., Golding, S. A.,

826   Hammer, R. B., Hanson, P. C., Johnson, P. T. J., Kamarainen, A. M., Kratz, T. K.,

827   Lathrop, R. C., McMahon, K. D., Provencher, B., Rusak, J. A., Solomon, C. T., Stanley,

828   E. H., Turner, M. G., Vander Zanden, M. J., … Yuan, H. (2007). Understanding

829   Regional Change: A Comparison of Two Lake Districts. *BioScience*, *57*(4), 323–335.

830   https://doi.org/10.1641/B570407

831 Catalán, N., Marcé, R., Kothawala, D. N., & Tranvik, Lars. J. (2016). Organic carbon

832   decomposition rates controlled by water retention time across inland waters. *Nature*

833   *Geoscience*, *9*(7), 501–504. https://doi.org/10.1038/ngeo2720

834 Cole, G., & Weihe, P. (2016). *Textbook of Limnology*. Waveland Press, Inc.

835   Cole, J. J., & Caraco, N. F. (1998). Atmospheric exchange of carbon dioxide in a low-wind

836   oligotrophic lake measured by the addition of SF $_6$. *Limnology and Oceanography*,

837   *43*(4), 647–656. https://doi.org/10.4319/lo.1998.43.4.0647

838 Cole, J. J., Carpenter, S. R., Kitchell, J. F., & Pace, M. L. (2002). Pathways of organic carbon

839   utilization in small lakes: Results from a whole-lake ^{13}C addition and coupled model.

840   *Limnology and Oceanography*, *47*(6), 1664–1675.

841   https://doi.org/10.4319/lo.2002.47.6.1664

842 Cole, J. J., Pace, M. L., Carpenter, S. R., & Kitchell, J. F. (2000). Persistence of net

843   heterotrophy in lakes during nutrient addition and food web manipulations. *Limnology*

844   *and Oceanography*, *45*(8), 1718–1730. https://doi.org/10.4319/lo.2000.45.8.1718

845

846   Creed, I. F., Sanford, S. E., Beall, F. D., Molot, L. A., & Dillon, P. J. (2003). Cryptic

847   wetlands: Integrating hidden wetlands in regression models of the export of dissolved

848   organic carbon from forested landscapes. *Hydrological Processes*, *17*(18), 3629–3648.

849   https://doi.org/10.1002/hyp.1357

850   Delany, A. (2022). *Modeled Organic Carbon, Dissolved Oxygen, and Secchi for six*

851   *Wisconsin Lakes, 1995-2014* [Data set]. Environmental Data Initiative.

852   https://doi.org/10.6073/PASTA/1B5B947999AA2F9E0E95C91782B36EE9

853   Dordoni, M., Seewald, M., Rinke, K., van Geldern, R., Schmidmeier, J., & Barth, J. A. C.

854   (2022). *Mineralization of autochthonous particulate organic carbon is a fast channel of*

855   *organic matter turnover in Germany's largest drinking water reservoir* [Preprint].

856   Biogeochemistry: Stable Isotopes & Other Tracers. https://doi.org/10.5194/bg-

857   2022-154

858   Evans, C. D., Monteith, D. T., & Cooper, D. M. (2005). Long-term increases in surface water

859   dissolved organic carbon: Observations, possible causes and environmental impacts.

860   *Environmental Pollution*, *137*(1), 55–71. https://doi.org/10.1016/j.envpol.2004.12.031

861   Feng, L., Zhang, J., Fan, J., Wei, L., He, S., & Wu, H. (2022). Tracing dissolved organic

862   matter in inflowing rivers of Nansi Lake as a storage reservoir: Implications for water-

863   quality control. *Chemosphere*, *286*, 131624.

864   https://doi.org/10.1016/j.chemosphere.2021.131624

865

866

867   Goudsmit, G.-H., Burchard, H., Peeters, F., & Wüest, A. (2002). Application of k-ε

868   turbulence models to enclosed basins: The role of internal seiches: APPLICATION OF

869   k-ε TURBULENCE MODELS. *Journal of Geophysical Research: Oceans*, *107*(C12),

870   23-1-23–13. https://doi.org/10.1029/2001JC000954

871   Hanson, P. C., Bade, D. L., Carpenter, S. R., & Kratz, T. K. (2003). Lake metabolism:

872   Relationships with dissolved organic carbon and phosphorus. *Limnology and*

873   *Oceanography*, *48*(3), 1112–1119. https://doi.org/10.4319/lo.2003.48.3.1112

874   Hanson, P.C., Carpenter S.R., Cardille, J.A, Coe, M.T., & Winslow, L.A. (2007). Small lakes

875   dominate a random sample of reginal lake characteristics. *Freshwater Biology* 52(5),

876   814–822. https://doi.org/10.1111/j.1365-2427.2007.01730.x

877   Hanson, P. C., Buffam, I., Rusak, J. A., Stanley, E. H., & Watras, C. (2014). Quantifying lake

878   allochthonous organic carbon budgets using a simple equilibrium model. *Limnology and*

879   *Oceanography*, *59*(1), 167–181. https://doi.org/10.4319/lo.2014.59.1.0167

880   Hanson, P. C., Hamilton, D. P., Stanley, E. H., Preston, N., Langman, O. C., & Kara, E. L.

881   (2011). Fate of Allochthonous Dissolved Organic Carbon in Lakes: A Quantitative

882   Approach. *PLoS ONE*, *6*(7), e21884. https://doi.org/10.1371/journal.pone.0021884

883   Hanson, P. C., Pace, M. L., Carpenter, S. R., Cole, J. J., & Stanley, E. H. (2015). Integrating

884   Landscape Carbon Cycling: Research Needs for Resolving Organic Carbon Budgets of

885   Lakes. *Ecosystems*, *18*(3), 363–375. https://doi.org/10.1007/s10021-014-9826-9

886   Hanson, P. C., Pollard, A. I., Bade, D. L., Predick, K., Carpenter, S. R., & Foley, J. A.

887   (2004). A model of carbon evasion and sedimentation in temperate lakes:

888   LANDSCAPE-LAKE CARBON CYCLING MODEL. *Global Change Biology*, *10*(8),

889   1285–1298. https://doi.org/10.1111/j.1529-8817.2003.00805.x

890

891 Hanson, P. C., Stillman, A. B., Jia, X., Karpatne, A., Dugan, H. A., Carey, C. C., Stachelek,

892   J., Ward, N. K., Zhang, Y., Read, J. S., & Kumar, V. (2020). Predicting lake surface

893   water phosphorus dynamics using process-guided machine learning. *Ecological*

894   *Modelling*, *430*, 109136. https://doi.org/10.1016/j.ecolmodel.2020.109136

895 Hart, J., Dugan, H., Carey, C., Stanley, E., & Hanson, P. (2019). *Lake Mendota Carbon and*

896   *Greenhouse Gas Measurements at North Temperate Lakes LTER 2016* [Data set].

897   Environmental Data Initiative.

898   https://doi.org/10.6073/PASTA/170E5BA0ED09FE3D5837EF04C47E432E

899 Hipsey, M. R. (2022). *Modelling Aquatic Eco-Dynamics: Overview of the AED modular*

900   *simulation platform*. https://doi.org/10.5281/ZENODO.6516222

901 Hipsey, M. R., Bruce, L. C., Boon, C., Busch, B., Carey, C. C., Hamilton, D. P., Hanson, P.

902   C., Read, J. S., de Sousa, E., Weber, M., & Winslow, L. A. (2019). A General Lake

903   Model (GLM 3.0) for linking with high-frequency sensor data from the Global Lake

904   Ecological Observatory Network (GLEON). *Geoscientific Model Development*, *12*(1),

905   473–523. https://doi.org/10.5194/gmd-12-473-2019

906 Hoffman, A. R., Armstrong, D. E., & Lathrop, R. C. (2013). Influence of phosphorus

907   scavenging by iron in contrasting dimictic lakes. *Canadian Journal of Fisheries and*

908   *Aquatic Sciences*, *70*(7), 941–952. https://doi.org/10.1139/cjfas-2012-0391

909   Hotchkiss, E. R., Sadro, S., & Hanson, P. C. (2018). Toward a more integrative perspective

910   on carbon metabolism across lentic and lotic inland waters. *Limnology and*

911   *Oceanography Letters*, *3*(3), 57–63. https://doi.org/10.1002/lol2.10081

912   Houser, J. N., Bade, D. L., Cole, J. J., & Pace, M. L. (2003). The dual influences of dissolved

913   organic carbon on hypolimnetic metabolism: Organic substrate and photosynthetic

914   reduction. *Biogeochemistry*, *64*(2), 247–269. https://doi.org/10.1023/A:1024933931691

915   Hunt, R. J., & Walker, J. F. (2017). *2016 Update to the GSFLOW groundwater-surface water*

916   *model for the Trout Lake Watershed*. https://doi.org/10.5066/F7M32SZ2

917   Hunt, R. J., Walker, J. F., Selbig, W. R., Westenbroek, S. M., & Regan, R. S. (2013).

918   *Simulation of Climate-Change Effects on Streamflow, Lake Water Budgets, and Stream*

919   *Temperature Using GSFLOW and SNTEMP, Trout Lake Watershed, Wisconsin*. United

920   States Geological Survey.

921   Jane, S. F., Hansen, G. J. A., Kraemer, B. M., Leavitt, P. R., Mincer, J. L., North, R. L., Pilla,

922   R. M., Stetler, J. T., Williamson, C. E., Woolway, R. I., Arvola, L., Chandra, S.,

923   DeGasperi, C. L., Diemer, L., Dunalska, J., Erina, O., Flaim, G., Grossart, H.-P.,

924   Hambright, K. D., … Rose, K. C. (2021). Widespread deoxygenation of temperate lakes.

925   *Nature*, *594*(7861), 66–70. https://doi.org/10.1038/s41586-021-03550-y

926   Jansson, M., Bergström, A.-K., Blomqvist, P., & Drakare, S. (2000). ALLOCHTHONOUS

927   ORGANIC CARBON AND PHYTOPLANKTON/BACTERIOPLANKTON

928   PRODUCTION RELATIONSHIPS IN LAKES. *Ecology*, *81*(11), 3250–3255.

929   https://doi.org/10.1890/0012-9658(2000)081[3250:AOCAPB]2.0.CO;2

930   Jenny, J.-P., Francus, P., Normandeau, A., Lapointe, F., Perga, M.-E., Ojala, A.,

931   Schimmelmann, A., & Zolitschka, B. (2016). Global spread of hypoxia in freshwater

932   ecosystems during the last three centuries is caused by rising local human pressure.

933   *Global Change Biology*, *22*(4), 1481–1489. https://doi.org/10.1111/gcb.13193

934   Jenny, J.-P., Normandeau, A., Francus, P., Taranu, Z. E., Gregory-Eaves, I., Lapointe, F.,

935   Jautzy, J., Ojala, A. E. K., Dorioz, J.-M., Schimmelmann, A., & Zolitschka, B. (2016).

936   Urban point sources of nutrients were the leading cause for the historical spread of

937   hypoxia across European lakes. *Proceedings of the National Academy of Sciences*,

938   *113*(45), 12655–12660. https://doi.org/10.1073/pnas.1605480113

939   Knoll, L. B., Williamson, C. E., Pilla, R. M., Leach, T. H., Brentrup, J. A., & Fisher, T. J.

940   (2018). Browning-related oxygen depletion in an oligotrophic lake. *Inland Waters*, *8*(3),

941   255–263. https://doi.org/10.1080/20442041.2018.1452355

942   Kraemer, B. M., Chandra, S., Dell, A. I., Dix, M., Kuusisto, E., Livingstone, D. M.,

943   Schladow, S. G., Silow, E., Sitoki, L. M., Tamatamah, R., & McIntyre, P. B. (2017).

944   Global patterns in lake ecosystem responses to warming based on the temperature

945   dependence of metabolism. *Global Change Biology*, *23*(5), 1881–1890.

946   https://doi.org/10.1111/gcb.13459

947   Ladwig, R., Hanson, P. C., Dugan, H. A., Carey, C. C., Zhang, Y., Shu, L., Duffy, C. J., &

948   Cobourn, K. M. (2021). Lake thermal structure drives interannual variability in summer

949   anoxia dynamics in a eutrophic lake over 37 years. *Hydrology and Earth System

950   Sciences*, *25*(2), 1009–1032. https://doi.org/10.5194/hess-25-1009-2021

951   Lathrop, R., & Carpenter, S. (2014). Water quality implications from three decades of

952   phosphorus loads and trophic dynamics in the Yahara chain of lakes. *Inland Waters*,

953   *4*(1), 1–14. https://doi.org/10.5268/IW-4.1.680

954   Lei, R., Leppäranta, M., Erm, A., Jaatinen, E., & Pärn, O. (2011). Field investigations of

955   apparent optical properties of ice cover in Finnish and Estonian lakes in winter 2009.

956   *Estonian Journal of Earth Sciences*, *60*(1), 50. https://doi.org/10.3176/earth.2011.1.05

957   Livingstone, D. M., & Imboden, D. M. (1996). The prediction of hypolimnetic oxygen

958   profiles: A plea for a deductive approach. *Canadian Journal of Fisheries and Aquatic*

959   *Sciences*, *53*(4), 924–932. https://doi.org/10.1139/f95-230

960   Loose, B., & Schlosser, P. (2011). Sea ice and its effect on CO_2 flux between the atmosphere

961   and the Southern Ocean interior. *Journal of Geophysical Research: Oceans*, *116*(C11),

962   2010JC006509. https://doi.org/10.1029/2010JC006509

963   Lovett, G. M., Cole, J. J., & Pace, M. L. (2006). Is Net Ecosystem Production Equal to

964   Ecosystem Carbon Accumulation? *Ecosystems*, *9*(1), 152–155.

965   https://doi.org/10.1007/s10021-005-0036-3

966   Maerki, M., Müller, B., Dinkel, C., & Wehrli, B. (2009). Mineralization pathways in lake

967   sediments with different oxygen and organic carbon supply. *Limnology and*

968   *Oceanography*, *54*(2), 428–438. https://doi.org/10.4319/lo.2009.54.2.0428

969   Magee, M. R., McIntyre, P. B., Hanson, P. C., & Wu, C. H. (2019). Drivers and Management

970   Implications of Long-Term Cisco Oxythermal Habitat Decline in Lake Mendota, WI.

971   *Environmental Management*, *63*(3), 396–407. https://doi.org/10.1007/s00267-018-

972   01134-7

973

974

Magnuson, J., Carpenter, S., & Stanley, E. (2020). *North Temperate Lakes LTER: Chemical*

   Limnology of Primary Study Lakes: Nutrients, pH and Carbon 1981 - current [Data set].

   Environmental Data Initiative.

   https://doi.org/10.6073/PASTA/8359D27BBD91028F222D923A7936077D

Magnuson, J. J., Benson, B. J., & Kratz, T. K. (2006). *Long-term dynamics of lakes in the*

   landscape: Long-term ecological research on north temperate lakes. Oxford University

   Press on Demand.

Magnuson, J. J., Carpenter, S. R., & Stanley, E. H. (2022). *North Temperate Lakes LTER:*

   Physical Limnology of Primary Study Lakes 1981 - current [Data set]. Environmental

   Data Initiative.

   https://doi.org/10.6073/PASTA/925D94173F35471F699B5BC343AA1128

McClure, R. P., Lofton, M. E., Chen, S., Krueger, K. M., Little, J. C., & Carey, C. C. (2020).

   The Magnitude and Drivers of Methane Ebullition and Diffusion Vary on a Longitudinal

   Gradient in a Small Freshwater Reservoir. *Journal of Geophysical Research:*

   Biogeosciences, *125*(3). https://doi.org/10.1029/2019JG005205

McCullough, I. M., Dugan, H. A., Farrell, K. J., Morales-Williams, A. M., Ouyang, Z.,

   Roberts, D., Scordo, F., Bartlett, S. L., Burke, S. M., Doubek, J. P., Krivak-Tetley, F. E.,

   Skaff, N. K., Summers, J. C., Weathers, K. C., & Hanson, P. C. (2018). Dynamic

   modeling of organic carbon fates in lake ecosystems. *Ecological Modelling*, *386*, 71–82.

   https://doi.org/10.1016/j.ecolmodel.2018.08.009

995

996 Mi, C., Shatwell, T., Ma, J., Wentzky, V. C., Boehrer, B., Xu, Y., & Rinke, K. (2020). The

997 formation of a metalimnetic oxygen minimum exemplifies how ecosystem dynamics

998 shape biogeochemical processes: A modelling study. *Water Research*, *175*, 115701.

999 https://doi.org/10.1016/j.watres.2020.115701

1000 Morris, M. D. (1991). Factorial Sampling Plans for Preliminary Computational Experiments.

1001 *Technometrics*, *33*(2), 161–174. https://doi.org/10.1080/00401706.1991.10484804

1002 Müller, B., Bryant, L. D., Matzinger, A., & Wüest, A. (2012). Hypolimnetic Oxygen

1003 Depletion in Eutrophic Lakes. *Environmental Science & Technology*, *46*(18), 9964–

1004 9971. https://doi.org/10.1021/es301422r

1005 Nürnberg, G. K. (1995). Quantifying anoxia in lakes. *Limnology and Oceanography*, *40*(6),

1006 1100–1111. https://doi.org/10.4319/lo.1995.40.6.1100

1007 Odum, H. T. (1956). Primary Production in Flowing Waters. *Limnology and Oceanography*,

1008 *1*(2), 102–117. https://doi.org/10.4319/lo.1956.1.2.0102

1009 Platt, T., Gallegos, C., & Harrison, W. (1980). Photoinhibition of photosynthesis in natural

1010 assemblages of marine phytoplankton. *Journal of Marine Research*, *38*(4), 687–701.

1011 Prairie, Y. T., Bird, D. F., & Cole, J. J. (2002). The summer metabolic balance in the

1012 epilimnion of southeastern Quebec lakes. *Limnology and Oceanography*, *47*(1), 316–

1013 321. https://doi.org/10.4319/lo.2002.47.1.0316

1014 Qu, Y., & Duffy, C. J. (2007). A semidiscrete finite volume formulation for multiprocess

1015 watershed simulation: MULTIPROCESS WATERSHED SIMULATION. *Water*

1016 *Resources Research*, *43*(8). https://doi.org/10.1029/2006WR005752

54

1017   Rautio, M., Mariash, H., & Forsström, L. (2011). Seasonal shifts between autochthonous and

1018   allochthonous carbon contributions to zooplankton diets in a subarctic lake. *Limnology*

1019   *and Oceanography*, *56*(4), 1513–1524. https://doi.org/10.4319/lo.2011.56.4.1513

1020   Read, E. K., Ivancic, M., Hanson, P., Cade-Menun, B. J., & McMahon, K. D. (2014).

1021   Phosphorus speciation in a eutrophic lake by 31P NMR spectroscopy. *Water Research*,

1022   *62*, 229–240. https://doi.org/10.1016/j.watres.2014.06.005

1023   Read, J. S., Hamilton, D. P., Jones, I. D., Muraoka, K., Winslow, L. A., Kroiss, R., Wu, C.

1024   H., & Gaiser, E. (2011). Derivation of lake mixing and stratification indices from high-

1025   resolution lake buoy data. *Environmental Modelling & Software*, *26*(11), 1325–1336.

1026   https://doi.org/10.1016/j.envsoft.2011.05.006

1027   Read, J. S., Zwart, J. A., Kundel, H., Corson-Dosch, H. R., Hansen, G. J. A., Vitense, K.,

1028   Appling, A. P., Oliver, S. K., & Platt, L. (2021). *Data release: Process-based*

1029   *predictions of lake water temperature in the Midwest US* [Data set]. U.S. Geological

1030   Survey. https://doi.org/10.5066/P9CA6XP8

1031   Reynolds, C. S., Oliver, R. L., & Walsby, A. E. (1987). Cyanobacterial dominance: The role

1032   of buoyancy regulation in dynamic lake environments. *New Zealand Journal of Marine*

1033   *and Freshwater Research*, *21*(3), 379–390.

1034   https://doi.org/10.1080/00288330.1987.9516234

1035   Rhodes, J., Hetzenauer, H., Frassl, M. A., Rothhaupt, K.-O., & Rinke, K. (2017). Long-term

1036   development of hypolimnetic oxygen depletion rates in the large Lake Constance.

1037   *Ambio*, *46*(5), 554–565. https://doi.org/10.1007/s13280-017-0896-8

1038   Richardson, D. C., Carey, C. C., Bruesewitz, D. A., & Weathers, K. C. (2017). Intra- and

1039   inter-annual variability in metabolism in an oligotrophic lake. *Aquatic Sciences*, *79*(2),

1040   319–333. https://doi.org/10.1007/s00027-016-0499-7

1041   Rippey, B., & McSorley, C. (2009). Oxygen depletion in lake hypolimnia. *Limnology and*

1042   *Oceanography*, *54*(3), 905–916. https://doi.org/10.4319/lo.2009.54.3.0905

1043   Schindler, D. W., Carpenter, S. R., Chapra, S. C., Hecky, R. E., & Orihel, D. M. (2016).

1044   Reducing Phosphorus to Curb Lake Eutrophication is a Success. *Environmental Science*

1045   *& Technology*, *50*(17), 8923–8929. https://doi.org/10.1021/acs.est.6b02204

1046   Snortheim, C. A., Hanson, P. C., McMahon, K. D., Read, J. S., Carey, C. C., & Dugan, H. A.

1047   (2017). Meteorological drivers of hypolimnetic anoxia in a eutrophic, north temperate

1048   lake. *Ecological Modelling*, *343*, 39–53.

1049   https://doi.org/10.1016/j.ecolmodel.2016.10.014

1050   Sobek, S., Tranvik, L. J., Prairie, Y. T., Kortelainen, P., & Cole, J. J. (2007). Patterns and

1051   regulation of dissolved organic carbon: An analysis of 7,500 widely distributed lakes.

1052   *Limnology and Oceanography*, *52*(3), 1208–1219.

1053   https://doi.org/10.4319/lo.2007.52.3.1208

1054   Soetaert, K., & Petzoldt, T. (2010). Inverse Modelling, Sensitivity and Monte Carlo Analysis

1055   in *R* Using Package **FME**. *Journal of Statistical Software*, *33*(3).

1056   https://doi.org/10.18637/jss.v033.i03

1057   Solomon, C. T., Bruesewitz, D. A., Richardson, D. C., Rose, K. C., Van De Bogert, M. C.,

1058   Hanson, P. C., Kratz, T. K., Larget, B., Adrian, R., Babin, B. L., Chiu, C.-Y., Hamilton,

1059   D. P., Gaiser, E. E., Hendricks, S., Istvànovics, V., Laas, A., O'Donnell, D. M., Pace, M.

1060   L., Ryder, E., … Zhu, G. (2013). Ecosystem respiration: Drivers of daily variability and

1061   background respiration in lakes around the globe. *Limnology and Oceanography*, *58*(3),

1062   849–866. https://doi.org/10.4319/lo.2013.58.3.0849

1063 Solomon, C. T., Jones, S. E., Weidel, B. C., Buffam, I., Fork, M. L., Karlsson, J., Larsen, S.,

1064   Lennon, J. T., Read, J. S., Sadro, S., & Saros, J. E. (2015). Ecosystem Consequences of

1065   Changing Inputs of Terrestrial Dissolved Organic Matter to Lakes: Current Knowledge

1066   and Future Challenges. *Ecosystems*, *18*(3), 376–389. https://doi.org/10.1007/s10021-

1067   015-9848-y

1068   Soranno, P. A., Carpenter, S. R., & Lathrop, R. C. (1997). Internal phosphorus loading in

1069   Lake Mendota: Response to external loads and weather. *Canadian Journal of Fisheries*

1070   *and Aquatic Sciences*, *54*(8), 1883–1893. https://doi.org/10.1139/f97-095

1071 Staehr, P. A., Bade, D., Van de Bogert, M. C., Koch, G. R., Williamson, C., Hanson, P.,

1072   Cole, J. J., & Kratz, T. (2010). Lake metabolism and the diel oxygen technique: State of

1073   the science: Guideline for lake metabolism studies. *Limnology and Oceanography:*

1074   *Methods*, *8*(11), 628–644. https://doi.org/10.4319/lom.2010.8.0628

1075 Steinsberger, T., Schwefel, R., Wüest, A., & Müller, B. (2020). Hypolimnetic oxygen

1076   depletion rates in deep lakes: Effects of trophic state and organic matter accumulation.

1077   *Limnology and Oceanography*, *65*(12), 3128–3138. https://doi.org/10.1002/lno.11578

1078 Thorp, J. H., & Delong, M. D. (2002). Dominance of autochthonous autotrophic carbon in

1079   food webs of heterotrophic rivers. *Oikos*, *96*(3), 543–550.

1080   https://doi.org/10.1034/j.1600-0706.2002.960315.x

57

1081   Toming, K., Kotta, J., Uuemaa, E., Sobek, S., Kutser, T., & Tranvik, L. J. (2020). Predicting

1082   lake dissolved organic carbon at a global scale. *Scientific Reports*, *10*(1), 8471.

1083   https://doi.org/10.1038/s41598-020-65010-3

1084   Tranvik, L. J. (1998). Degradation of Dissolved Organic Matter in Humic Waters by

1085   Bacteria. In D. O. Hessen & L. J. Tranvik (Eds.), *Aquatic Humic Substances* (Vol. 133,

1086   pp. 259–283). Springer Berlin Heidelberg. https://doi.org/10.1007/978-3-662-03736-

1087   2_11

1088   Webster, K. E., Kratz, T. K., Bowser, C. J., Magnuson, J. J., & Rose, W. J. (1996). The

1089   influence of landscape position on lake chemical responses to drought in northern

1090   Wisconsin. *Limnology and Oceanography*, *41*(5), 977–984.

1091   https://doi.org/10.4319/lo.1996.41.5.0977

1092   Wilkinson, G. M., Pace, M. L., & Cole, J. J. (2013). Terrestrial dominance of organic matter

1093   in north temperate lakes: ORGANIC MATTER COMPOSITION IN LAKES. *Global*

1094   *Biogeochemical Cycles*, *27*(1), 43–51. https://doi.org/10.1029/2012GB004453

1095   Williamson, C. E., Dodds, W., Kratz, T. K., & Palmer, M. A. (2008). Lakes and streams as

1096   sentinels of environmental change in terrestrial and atmospheric processes. *Frontiers in*

1097   *Ecology and the Environment*, *6*(5), 247–254. https://doi.org/10.1890/070140

1098   Winslow, L. A., Zwart, J. A., Batt, R. D., Dugan, H. A., Woolway, R. I., Corman, J. R.,

1099   Hanson, P. C., & Read, J. S. (2016). LakeMetabolizer: An R package for estimating lake

1100   metabolism from free-water oxygen using diverse statistical models. *Inland Waters*,

1101   *6*(4), 622–636. https://doi.org/10.1080/IW-6.4.883

1102